ADDIS ABABA UNIVERSITY

COLLEGE OF TECHNOLOGY AND BUILT ENVIRONMENT

SCHOOL OF CIVIL AND ENVIRONMENTAL ENGINEERING

Truss Reinforcement vs. Conventional Arrangements of stirrup for Enhancing Shear Capacity of Slender beams.

A Thesis in Structural Engineering

BY TAMRAT ALI

December 4, 2025

Addis Ababa

A Thesis

Submitted in Partial Fulfillment of the Requirements for the Degree of Master of Science

The undersigned have examined the thesis entitled '**Truss Reinforcement vs. Conventional Arrangements of stirrup for Enhancing Shear Capacity of Slender beams.'** presented by **Tamrat Ali**, a candidate for the degree of **Master of Science** and hereby certify that it is worthy of acceptance.

Dr. Esayas G/Youhannes		Dec-25-25
Advisor	Signature	Date
Dr. Abrham Gebre		Dec. 08/2025
Internal Examiner	Signature	Date
Dr. Birhanemeskel Engliz		Dec. 23/2025
External Examiner	Signature	Date
Dr. Yenesew Mengistu		Dec 24/2025
Chairperson	Signature	Date

School of Civil & Environmental Engineering
College of Technology and Built Environment
Addis Ababa University

UNDERTAKING

I certify that research work titled "**Truss Reinforcement vs. Conventional Arrangements of stirrup for Enhancing Shear Capacity of Slender beams.**" is my own work. The work has not been presented elsewhere for assessment. Where material has been used from other sources it has been properly acknowledged/referred.

Tamrat Ali

Signature

Date December 4, 2025

ABSTRACT

This study investigates the importance of using truss reinforcement stirrup arrangement as an alternative to Conventional vertical stirrups as the shear reinforcement in slender reinforced concrete (RC) beams. The goals of the study are to experimentally investigate the shear behavior and failure modes of slender RC beams with stirrups arranged in truss form compared to beams reinforced with Conventional stirrups, and to develop numerical models using Abaqus that would simulate beam shear behavior and to verify the numerical models with the experimental results of the beams based on comparisons of load capacity, crack patterns, and failure modes and to select the best inclination angle. The experimental phase involves castings of three slender RC beams with the same dimensions, same materials and same load configurations, but with different stirrup configurations (Conventional vertical stirrups, non-staggered Warren truss stirrup, staggered Warren truss stirrup). And set the surface monitoring system with transducers to monitored shear strain at the left side of the front face of each beam. This study investigated the effectiveness of truss reinforcement to replace conventional vertical stirrups as shear reinforcement in slender reinforced concrete (RC) beams. The study objectives: experimentally investigating shear behavior and failure modes of slender RC beams with stirrups configured in truss form in comparison to beams using conventional stirrups. In the FEM study, five different models were used, including the conventional stirrup model and truss types with two different inclination angles of 45° and 57°. The findings revealed that all beams failed by shear mode, where the beams with the truss stirrups with 57^0 inclined exhibited higher ultimate shear strength than the beams with conventional stirrups. The non-staggered truss stirrups with 57^0 inclined had 18.25 % improvement for experimental ultimate load and 31.09 % improvement predicted using FEM. The staggered truss configuration with 57^0 inclined was shown to have the largest improvement with experimental ultimate load improvement of 26.75% improvement and FEM capacity increment of 32.89%. The staggered truss stirrups with 57^0 inclined were determined to be the most beneficial stirrup arrangement for improving shear strength. In FEM analysis, non-staggered and staggered truss stirrups inclined at 45° exhibit lower shear capacity than all other truss types and conventional stirrups, as observed in both experimental and FEM results.

Keywords: Truss reinforcement, Shear capacity, Slender reinforced concrete beams, Stirrup arrangement, Finite element analysis, transducers

ACKNOWLEDGMENTS

First of all, I want to thank God for his blessings and for guiding me through every success I've had in my life. And I want to thank my family for their love and support throughout my personal life and in my professional career.

I would like to express my deepest appreciation to my advisor, who became my role model and source of motivation, Dr. Esayas G/Youhannes, for his guidance, continued support and remarkable patience, all the way through my research. His trust and confidence in me has allowed me to take this challenge and succeed.

My deepest thanks go to all the Civil and Environmental Engineering Department of Addis Ababa University instructors for their guidance and support to this research and the non-teaching staff.

I am also thankful to all AAiT Construction Material Laboratory staff members for their cooperation and help during the experimental program and to my family their financial support and inspiration from the beginning to the end of the work.

Table of Content

List of Table

List of Figure

LIST OF ABBREVIATIONS

ACI	American concrete institute
JSCE	Japan Society of Civil Engineers
AAiT	Addis Ababa Institute of Technology
BS EN	British Standard European Norm
ES EN	Ethiopian Standard European Norm
LVDT	Linear Variable Displacement Transducer
OPC	Ordinary Portland Cement
RC	Reinforced Concrete
DSR	diagonal shear reinforcement
FEM	Finite element Method
CDP	Concrete damaged plasticity
CB	Control beam
TBNS	Truss Beam Non-Staggered
TBS	Truss Beam Staggered
NRSB	non-welded rectangular stirrup beam
WRSB	welded rectangular stirrup beam
NWWTB	normal welded warren truss shaped beam
FWWTB	flipped welded warren truss shaped beam

LIST OF SYMBOLS

f_c'	Compressive strength
Ø	Diameter of rebar
A_s	Area of steel
a	Shear span
d	Effective depth
f_y	Yield Strength
f_{ct}	Tensile strength
f_{ctd}	Design concrete tensile strength
c	Concrete Cover
P	Maximum load
ρ_1	Reinforcement ratio for longitudinal reinforcement
M_d	Design moment
$V_{Rd,s}$	Design shear capacity
f_{ywd}	yield strength of web reinforcement

CHAPTER ONE

1. INTRODUCTION

1.1 Background of The Study

A beam is a structural Element that Carries External applied loads and its own weight mainly through bending moments and shears**[1].** Reinforced concrete (RC) beams are essential components of structures and civil infrastructures, and are mostly Affected by bending and shear forces. Shear occurs within a beam as an internal transverse force that acts parallel to the cross-section of the beam due to the External transverse load on the beam. Shear occurs when forces acting on the beam enable adjacent layers to slide and create shear stresses within the material. Shear forces are usually greatest near the supports in the span of the beam and can lead to shear failure, especially where diagonal cracks form. The shear force in the beams is resisted by the concrete itself, transverse reinforcement (stirrups), and the bond between concrete and longitudinal reinforcement. The shear behavior in reinforced concrete (RC) beams is quite complex. It is due to the non-homogeneity, cracking, reinforcements, and the material's nonlinear response. The manner in which shear failure occurs widely depends on geometry, Type of load which we apply, and the material's properties.

The distribution of the shear stress in reinforced concrete beams is not well known, and the distribution of shear stresses throughout the cross-section is not well defined. Therefore, there is no single Approach to design for shear **[1]**.

In reinforced concrete Beams, stirrups are Inserted for resisting shear, as well as to Resist diagonal cracking and shear failure of the beam. conventional stirrups, which constructed mainly in the form of closed loop transverse ties, satisfactorily Distribute shear in cracked concrete members. However, in slender beams where the span to depth ratios are high their performance is negatively impacted owing to early diagonal cracking, poor aggregate interlock, and intricate crack patterns. Aside from that, congested stirrup arrangements also make concrete casting and compaction more difficult, resulting in inferior quality and increased labor costs. Some Studies in structural engineering also foresee other reinforcement techniques having superior performance, particularly in beams under high shear. They include the truss model concept, in which diagonal reinforcements are arranged to produce a truss like mechanism within the beam, following the direction of the internal forces. By substituting the conventional stirrups with a truss system of reinforcement, the mechanism of shear resistance is more straightforward by trending along principal directions of stress and can improve the shear capacity of slender beams.

A truss is an assembly of straight members joined at nodes forming simple arrangements mainly in the shape of triangular units. Truss provides stability leading to effective load transfer that is mostly performed in axial forces, either in tension or compression. Their strength and utilization of material efficiently, have made trusses the assembly type of choice for bridges, roofs, towers and other structures.

In RC beams, if the patterns of reinforcement are upgraded as any one of the trusses, the improved behavior is possible to ensure. That is just such an attempt is made here.

1.1.1 Some Types of Trusses

1.1.1.1. Howe Truss

In the Howe truss, the diagonal members are in compression and the vertical members are in tension. The Howe truss is most effective for longer spans and heavier loads; for example, large bridges or a large roof structure. Designing to prevent buckling can be helped with compressive diagonals. In some situations, this can be a unique structural advantage.

1.1.1.2. Pratt Truss

The Pratt truss is essentially the reverse of the Howe truss and is a very common type of structural system commonly used in bridges with medium to long spans. The Pratt truss has vertical members under compression and diagonal members under tension, with diagonals typically sloping toward the center of the span.

1.1.1.3. Warren Truss

The Warren truss is characterized by diagonal members, that create equilateral or isosceles triangles. The diagonals alternate in direction which equalizes the forces put on the truss components with tension and compression. This uncomplicated system also minimizes structural components and connections, thereby providing an economical solution for either bridge or roof spans of moderate length. In summary, each truss shape has its own unique geometrical or structural benefits, making their selection a function of span, loading conditions, economy and aesthetics.

This research has selected the Warren truss as a preferred truss shape over all other truss shapes due to its practical and static efficient methodology for designing reinforced concrete beams. It is designed to utilize the least material and end up being the least expensive and produce a reasonable performance in practice. While there are other truss systems, the Warren truss outperforms the other configurations in both economy and efficiency in its use of materials, therefore is the preferred alternative for most RC beam applications.

1.2. Statement of the Problem

Efficient configuration of stirrups for enhanced shear performance is a subject of research in structural Engineering. One of the main challenges in structural engineering is figuring out the best shear reinforcement configuration to increase the shear capacity of Slender reinforced concrete beams. Though alternative truss-shaped stirrup systems may offer better shear resistance, conventional stirrup arrangements are still commonly used. In order to determine the best technique for increasing the shear capacity of slender beams, this study examines and contrasts the shear strength performance of truss reinforcement with Conventional stirrups.

This research focuses on the following primary queries: -

- Does the truss stirrup pattern provide better shear performance when compared to conventional vertical stirrups in slender RC beams?
- How does changing the stirrup arrangement impact crack propagation, deflection behavior, and ultimate load capacity?
- Do numerical models accurately predict what was observed in the experimental testing and to identify which inclination angle is the best?

Through addressing these questions, this research aims to provide guidance towards developing improvements to the existing shear design approach to reinforced concrete with different stirrup configuration, as well as, formulating guidance to improve shear reinforcement detailing and improved practices in slender beam applications.

1.3. Research Objectives

The main aim of this study will be to explore the capabilities of truss reinforcement as an alternative to conventional stirrups to provide shear capacity to slender RC beams for structural performance.

1.3.1. Specific objectives

- To experimentally investigate slender beams of reinforced concrete in shear and their failure modes when stirrups are arranged in trusses, and compare this with conventional stirrups.
- To develop a numerical model that performs a simulation of the shear of slender beams with stirrups of truss arrangement when subjected to loading.
- To compare and validate the Numerical model against the experimental test results based on load capacity, cracks pattern and failure modes.

1.4. Significance of the Study

Shear failure in RC Slender beams often occurs abruptly and catastrophically thus, structural design must identify ways to avoid this. Other methods of reinforcement like truss particulars may prove beneficial given the advancement of design philosophies and the need for safer, cheaper, and more efficient structures. This research paper evaluated the performance of truss and conventional stirrup configurations in slender beams, specifically looking at how they improved shear strength, crack control, and failure mode behavior. The results provide insight that will help structural engineers optimize details for reinforcement for shear critical elements, while also informing design guideline.

The research provides an understanding of how new stirrup configurations, specifically truss arrangements, affect the shear behavior of slender beams.

1.5. Scope of the Study

The focus of this study is the behavior of slender reinforced concrete beams when subjected to shear forces. The study will examine how changing the stirrup arrangement can have an effect on shear strength and failure modes. The study seeks to compare the beams designed with conventional vertical stirrups to beams designed with more truss like stirrup arrangements, to see if some increase in shear capacity can be achieved as a result of the truss shapes. The study uses a combination of experimental Three-point bending tests and numerical finite element analysis. Experiments will allow to develop further understanding of structural behavior in this scenario, allowing the researchers to compare the results from the tests directly with predictions from the finite element models.

The proposal is deliberately limiting beam design to standard materials, with standard concrete strength and reinforcement ratios to exclude any effects from specialized materials. The study also does not consider dynamic effects, such as impacts or loading cycles, with the investigation limited only to static loading. The study's results can ultimately be translated into recommendations for the use of truss arrangements as shear stirrups.

The research method is consistent with the body of literature, which suggests that truss stirrup patterns can lead to substantial improvements in strength. This study mainly focused on rigorously combine experimental and numerical analysis to obtain accurate and validated results.

1.6. Methodology

This research employs experimental and numerical methods to evaluate the effects of various stirrup designs on the shear capacity of slender reinforced concrete beams. Three beams with the same dimensions and the same amount materials are used in the experiment. Similar concrete mix and reinforcement used throughout the beams will ensure that the only variable is stirrup configuration.

For Experimental work the first beam is considered the control and the stirrups are conventional vertical stirrups to simulate shear reinforcement as in a traditional situation. The second beam applied a non-staggered Warren truss stirrup (with 57^0 inclined) configuration and the last beam employed a staggered Warren truss stirrup (with 57^0 inclined).

in Numerical Analysis There are five models three of them are the same with the experimental, the other two models are a non-staggered Warren truss stirrup (with 45^0 inclined) and a staggered Warren truss stirrup (with 45^0 inclined) configuration respectively.

After casting and curing, all three beams were tested in the laboratory of AAIT in three-point bending. They were tested until ultimate loads were achieved while helping identify three critical behaviors in shear loading, which include the initiation and extension of shear cracks, the load and deflection responses physically observed, and finally, the ultimate mode of failure. Use of the experimental procedure equipped with data logger, load cell, and displacement transducers allows for accurate measurements of both load and deformation taken throughout the course of the tests.

Finite element models of each beam are established in ABAQUS to complement the experimental stage. Each finite element model replicates the physical specimens in terms of geometry, reinforcement detailing, material properties, boundary conditions, and loading. Each finite element model has also employed nonlinear constitutive models for concrete and Reinforcement to realistically with cracking and yielding due to shear loading.

Comparisons between numerical results and experimental results include load capacity, deflection behavior, crack development, and failure mechanisms. This validation will confirm the correlativity of the numerical model and allow for further parametric studies later if required.

Ultimately, combining experimental testing with advanced numerical modelling will offer clarity on the effect of conventional, non-staggered Warren truss, and staggered Warren truss stirrup arrangements on the shear performance of slender reinforced concrete beams.

CHAPTER TWO

2. LITERATURE REVIEW

This chapter presents a summary of the literature relevant to improving the shear capacity of slender reinforced concrete beams through different stirrup arrangements. Specifically, the review is segmented into Three categories: first, sections from experimental studies that explored different stirrup configurations; second, numerical studies that assessed shear resistance capacity in beams with different stirrup arrangements. and third, various design codes. This structure establishes a wide scope of the ways and methods of improving shear behavior in slender beams.

2.1. Experimental Investigations on Shear Capacity with Alternative Stirrup Arrangements

2.1.1. Impact of Swimmer or inclined Shear Reinforcement on RC Beam Performance

The study undertaken by Nasra and Asha in 2013**[20]** establishes the performance of shear capacity by using four types of shear reinforcement Arrangements in reinforced concrete beams those are conventional stirrups, welded swimmer bars, bolted swimmer bars, and U-link bolted swimmer bars as shown in Fig. **2-1**. The findings revealed that beams with swimmer bars have a greater shear capacity compared to the control beams. Beams reinforced with welded swimmer bars exhibited similar strength to U-link bolted swimmer bars and bolted swimmer bars, indicating that welding could be avoided when using swimmer bars. it is advantageous to use swimmer bars to improve shear capacity. Khan et al. in 2015**[11]** assessed the effectiveness of swimmer bars as an alternative to the conventional vertical stirrup for providing shear reinforcement in reinforced concrete beams. The swimmer bars were placed at a 45-degree angle in the experimental study as shown in Fig. **2-2**, and were connected to the main longitudinal reinforcement. the beams that used swimmer bars increased shear strength and stiffness compared to beams that used vertical stirrups, and the beams that utilized swimmer bars needed larger spacing between the reinforcement elements without any negative impacts on the structural performance. In addition, the beams that had swimmer bars achieved higher ultimate load capacity and had fewer cracks resulting in greater durability and overall structural behavior.

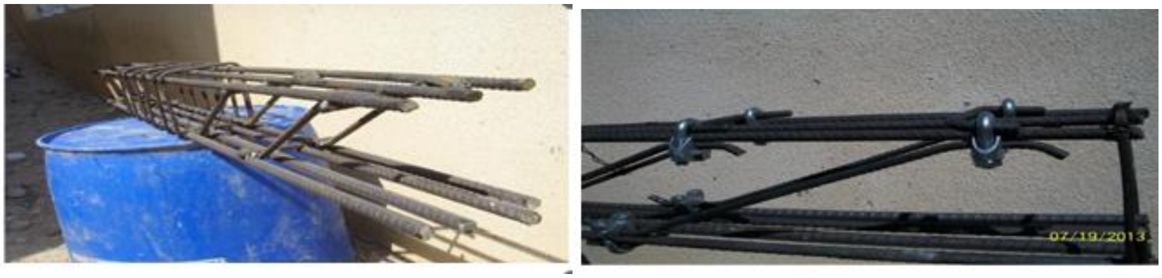

Fig. 2-1 Welded and U-link bolted swimmer bars [20].

Fig. 2-2 Single and legged swimmer bar respectively [11].

Colajanni, P., et al in 2014**[8]** introduced an advanced model for estimating the shear capacity of reinforced concrete beams with web reinforcement, expanding upon the classical plastic Nielsen model by incorporating a variable-inclination stress-field methodology. The proposed approach demonstrates robust predictive capabilities for the shear strength of beams featuring stirrups arranged at two distinct angles, as well as those reinforced with longitudinal web bars. Suhaimi et al. in 2015**[9]** studied on the use of inclined links as shear reinforcement in reinforced concrete (RC) beams, looked at alternatives to the conventional vertical stirrups, The beams with inclined links had shear capacities that were approximately 18% to 33% greater than the beams reinforced with vertical stirrups. Mohamed et al. in 2018**[7]** performed an experimental investigation to examine the effect of inclined shear reinforcement on the response of reinforced concrete (RC) beams, in contrast to conventional vertical stirrups. Two RC beam specimens were constructed the ultimate load for the inclined beam was 250kN while the beam with vertical stirrups had an ultimate load of 207kN. Both specimens eventually failed in shear compression. These results suggest that inclined shear reinforcement is more effective at increasing both shear capacity and ductility of RC beams; and therefore, could be a practical alternative to vertical stirrups. The experimental results were confirmed by comparing the results with Eurocode 2 predictions, further supporting reliability. Colajanni et al. in 2020**[17]** derived a physical model which generalizes the Eurocode 2 way of using the static theorem of plasticity to explore two orders of transverse reinforcement, tolling, with the aim of determining equations for selecting optimum parameters and plastic admissibility. Their mechanistic model, which was verified against experimental results, described both shear and chord failure and verified the use of inclined stirrups, especially the 45° inclination, compared to traditional vertical stirrups. In addition, the model allows for mapping of homogeneous behavioral zones through the use of specific reinforcement ratios facilitating careful design schemes according to case requirements. Ultimately, this approach spans both extending design code utility and provides analytical means to attain greatest optimization of reinforcement layouts.

2.1.2. Impact of Truss Shear Reinforcement on RC Beam Performance

Grandić, D., et al in 2015**[2]** studied the shear resistance of reinforced concrete beams as a function of concrete strength in compressive struts utilizing a truss model with adjustment angles of inclination of the struts varying from 21.8° to 45°. A parametric study compares different design approaches including European code EN 1992-1-1, German DIN, and Canadian design approaches predicting maximum shear resistance as a function of compressive strength and angle of inclination of the concrete struts .Mahzuz, H. M. A., et al. in 2021**[3]** Carried out an experiment aimed at investigated the shear strength and ultimate load capacity of traditional reinforced concrete beams as opposed to alternative reinforcement combinations as shown in Fig. **2-3**, **2-4, 2-5 and 2-6.** This Study was used welded rectangular stirrup beam (WRSB); non-welded Warren truss beam (NWTB) and welded Warren truss beam (WWTB). the welded Warren truss beam (WWTB) provided the highest shear strength increases and ultimate loads.

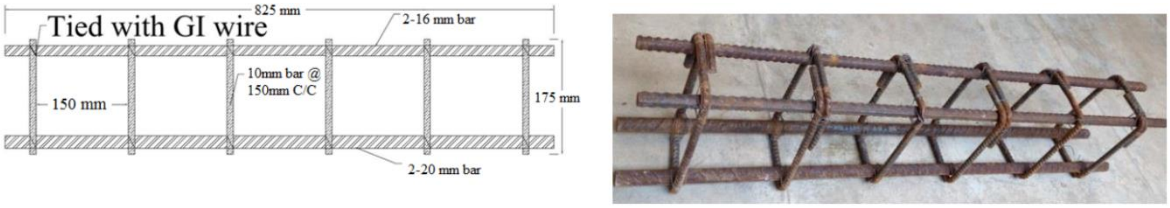

Fig. 2-3 Non welded rectangular truss beam [3].

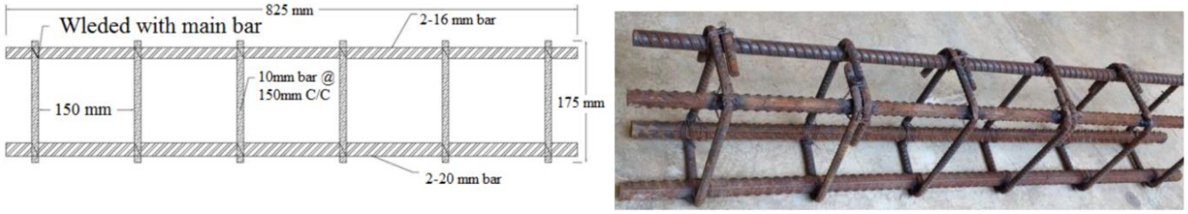

Fig. 2-4 Welded rectangular truss beam [3].

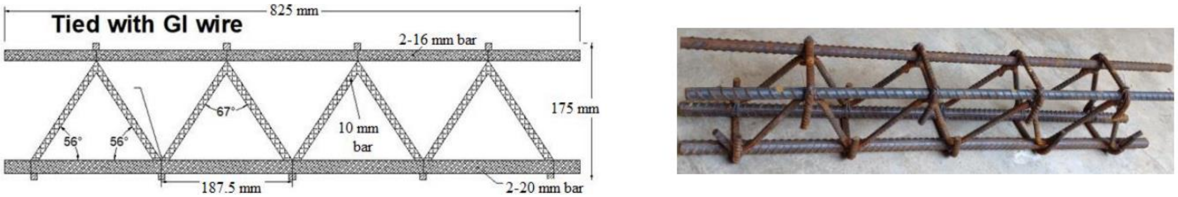

Fig. 2-5 Non welded warren truss beam [3].

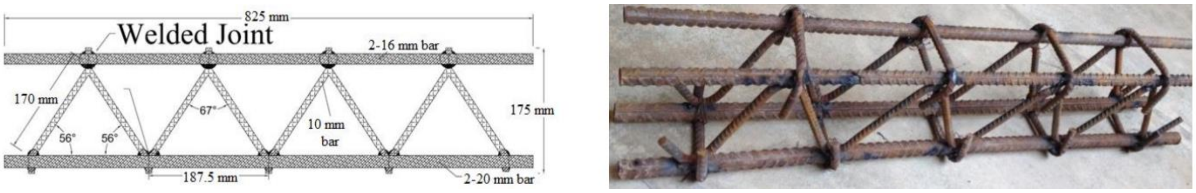

Fig. 2-6 Welded warren truss beam [3].

Djamaluddin et al. 2014**[10]** studied new forms of structural systems, one being to provide a beam with a truss system when there is no concrete provided in the beam's tension zones. This study specifically compared externally reinforced truss systems that were tested, and nearly achieved the same flexural capacities of beams having tension zones completely composed of concrete. The truss-reinforced beams also had fewer cracks, presumably due to better control over the tensile reinforcement that helps limit the crack propagation, nonetheless the research mainly examines flexural strength without an in-depth exploration of shear behavior or combined shear-flexure behavior. Saju et al. 2016**[13]** studied the flexural strength of reinforced concrete beams, focusing on two types of steel truss reinforcement configurations as depicted in Fig. **2-7** of their publication. Their experimental observations demonstrated that beams utilizing truss reinforcement achieved approximately a 20% increase in ultimate failure load compared to those with conventional vertical stirrups. The beams with truss reinforcements are less deflected during the service stage, However, the study focuses on flexural strength without a detailed investigation of shear behavior or combined shear-flexure behavior.

Fig. 2-7 reinforcement pattern 1 and 2 respectively [13]

Laurens Frans et al. in 2019**[15]** investigated whether adjustment to the reinforcement configuration in concrete beams would enhance the flexural performance of concrete beams. The study tested six beams in total, with three beams containing conventional vertical ties and three beams that contained ties arranged in a truss configuration. The flexural testing produced a maximum load for the truss beams that was significantly larger than the maximum load for normal beams that contained vertical ties. The truss beams also deflected less under service loads, which indicated that the truss beams were more stiff and stronger overall than the normal beams. Pinto et al. in 2022**[18]** studied the experiments tested the effectiveness of pre-fabricated truss stirrups as the main shear reinforcement, in combination with supplemental reinforcement to control cracks due to delamination. with shear strength improvements up to 142% due to the use of pre-fabricated truss stirrups, demonstrating their significant contribution to improving structural capacity. Experimental results were also compared with theoretical shear strength calculations from a number of design codes - NBR 6118 (2014), Eurocode 2 (2004), and ACI 318 (2014) - as part of the confirmation of the factors of safety and acceptability of the design codes for concrete members reinforced in the manner investigated.

2.1.3. Effect of shear span to depth ratio on shear capacity of RC beams

The ratio of shear span to depth (a/d) is an important factor in the shear capacity of reinforced concrete (RC) beams. A shear span to depth ratio (a/d) is an important parameter that influences shear failure of beams. Bukhari and Ahmad in 2007**[36]** explored this parameter on the mechanisms of failure and discovered that the shear strength increases as the a/d ratio decreases. In the study, the authors varied the a/d ratio from 1 to 4. It was found that increasing the a/d ratio from 2 to 3 reduces the relative flexural strength of the beam; however, this was also dependent on the amount of tensile reinforcement in the beam. The a/d ratios that are between 1.5 and 2.5 would lead to inclined cracks developing prior to failure. Ahmad and Gasham in 2011**[35]** focused on the shear capacity equations for cases of a/d greater than or equal to a value of 2, and developed a capacity equation that more realistically represents the behavior of beams at the onset of shear cracking. Hunegnaw, C. B., & Wondimu, T. (2021)**[38]** research examines the influence of stirrup orientation on the shear capacity of reinforced concrete (RC) beams, focusing mainly on the effects of different shear-span-to-depth ratios (a/d).

2.1.4. variation of Concrete Grade with the same reinforcement ratio regard with shear capacity

Mahzuz, H. M. A., et al. in 2021**[3]** Carried out an experiment aimed at investigated the shear strength and ultimate load capacity of traditional reinforced concrete beams as opposed to alternative reinforcement combinations, This Study was used welded rectangular stirrup beam (WRSB); non-welded Warren truss beam (NWTB) and welded Warren truss beam (WWTB). Each type was defined by the stirrup orientation, with all beams designed with the same amount of reinforcement and the same amount of concrete all presumed cost hadn't been a problem. The experimental results shown as follow, The WRSB showed a 17.6% increase in ultimate load over the non-welded rectangular stirrup beam (NRSB) for the 1:1.5:1.5 concrete mix, NWTB improved 14.9%, and WWTB had a 34.2% increase over NRSB. Overall, even after mixed conditions were used to evaluate the beams performance, a leaner concrete mix (1:2.5:2.5) demonstrated an increase of 17.3% from WRSB drone to NRSB, 11% from NWTB and a 30.2% increase from WWTB. On average, the 1:3:3 mix produced shear strength increases of 18% from WRSB to NRSB, 12.17% from NWTB to NRSB, and 32.01% from WWTB to NRSB. In all tests and mix comparisons, the welded Warren truss beam (WWTB) provided the highest shear strength increases and ultimate loads. Additionally, the qualitative ranking of the four types of beams (in all configurations and mixes) did not change: NRSB was the worst, NWTB was second worst, WRSB was third, and WWTB (Welded Warren Truss Beam) is always showed the best performance.

2.1.5. Limitations of Experimental Studies

As mentioned in the prior literature review, many experimental studies focus on inclined and truss reinforcement arrangements instead of the conventional vertical stirrups to increase the shear capacity of the reinforced concrete beams. These studies mostly focus on beams with shear span to depth (a/d) ratios of less than 2, which are short beams and further challenges to generalize to more slender beams used in practice in general. This context indicates a clear research gap concerning inclined or truss stirrups configurations in beams with greater a/d ratios.

2.2. Numerical Investigations on Shear Capacity with Alternative Stirrup Arrangements

2.2.1. Overview of the Impact of Inclined and Truss Stirrup Arrangements on RC Beam Capacity through Numerical Modeling

Using a validated finite element model in ANSYS 14.5, Kishori and Philip in 2014**[21]** studied the effectiveness of swimmer bars as a substitute shear reinforcement in rectangular reinforced concrete beams. The research focused on versatile arrangements of swimmer bars, single bars, rectangular, and those with cross bracing or vertical and horizontal partitioning, and evaluated their effects on deflection, shear capacity, and crack pattern progression. Demir et al. in 2016**[22]** suggested implementing diagonal shear reinforcement (DSR) which, as illustrated in Fig. **2-8**, enhanced the shear strength of beams by as much as 86.7%. Furthermore, the application of DSR improves the ductility capacity of reinforced concrete beams. In addition, the study indicated that increased DSR diameters alongside higher yield strengths enhanced the shear capacity so much that the failure mode transitioned from shear failure to flexural failure**.**

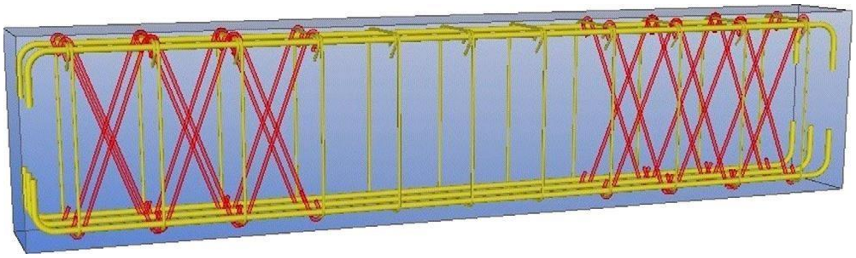

Fig. 2-8 Diagonal shear reinforcement [22].

Deepika Dinesh, A., et al in 2017**[12]** examined reinforced steel trussed concrete beams through numerical examination that investigated the area where steel truss systems and reinforced concrete interrelate to improve structural performance. Using ANSYS software, they evaluated that adding steel truss elements into concrete beams improves pressure and shear resistance, reduces overall beam deflection, and delayed crack propagation. Arafa, M., et al in 2018**[5]** studied the shear performance of reinforced concrete beams with embedded steel trusses under small shear span-to-depth (a/d) ratios by utilizing nonlinear finite element models in ABAQUS. The result of this study indicated a substantial increase in ultimate shear strength, as much as 98% at a/d = 1. Afefy, H., et al in 2022**[6]** conducted the behavior of reinforced concrete beams, which consisted of embedded steel trusses as web reinforcement, instead of conventional vertical stirrups. They compared the beams to the standard designs and demonstrated with finite element modelling using the ABAQUS software different beam configurations, representing different amounts of shear reinforcement. The authors of the paper concluded that the beams that had steel trusses in the beams had up to a 4% to 8% higher ultimate load capacity, improved crack control, and more ductile failure modes. These findings indicate that internal steel trusses can effectively improve Flexural strength and stiffness, and could be an effective replacement for stirrups. Nazia Sultana et al in 2022**[14]** conducted a study by using different truss configurations (Pratt, Howe, and Warren trusses) as internal reinforcement in ABAQUS. The study did not use standard rebar, but instead implemented steel square bars in truss configurations to see how the truss reinforced beams would perform comparatively in terms of load capacity, total energy absorbed prior to failure, and amount of stress they could withstand under similar loading prior to failure. The results were particularly promising for the Howe truss configuration, which was shown to be effective to an extraordinary degree. The Howe truss-reinforced beam withstood an ultimate load of 7kN, a very stark improvement over the control beam at 0.24kN.

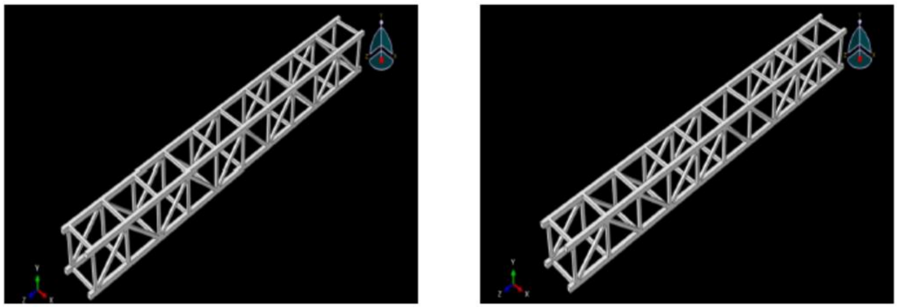

Fig. 2-9 Warren and Pratt truss arrangement respectively [14].

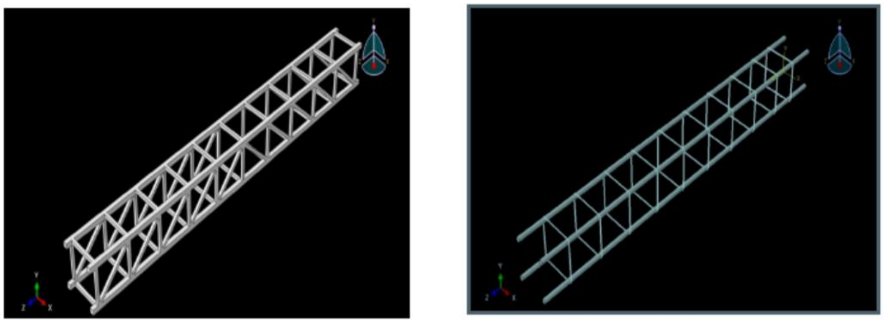

Fig. 2-10 Howe truss and conventional arrangement respectively [14].

Gungat, L., et al in 2024**[16]** examined the influence of the variations within stirrup configurations on the behavior of reinforced concrete beams using Finite Element Modelling in Abaqus. There were a total of seventeen different models that covered traditional configurations, spiral types, and truss styles as well as more advanced or unique stirrup configurations The research assessed behavior stages like load deflection responses, strength, ductility, failure modes and crack propagation. This paper shows the clear advantages to the use of modified stirrup designs that can increase beam capacity and lead to superior failure modes and crack control. Juhin, W.J., et al in 2024**[4]** conducted on the torsional performance of reinforced concrete beams with non-welded rectangular stirrup beam (NRSB), welded rectangular stirrup beam (WRSB), normal welded Warren truss shaped beam (NWWTB), and flipped welded Warren truss shaped beam (FWWTB) by using ANSYS software. All beams had the same dimensions and reinforcement weight and two compressive strengths of (22.92 MPa and 43.47 MPa) were tested. The study showed that the WRSB configuration had the highest torsional moment capacity when compared to the other beams.

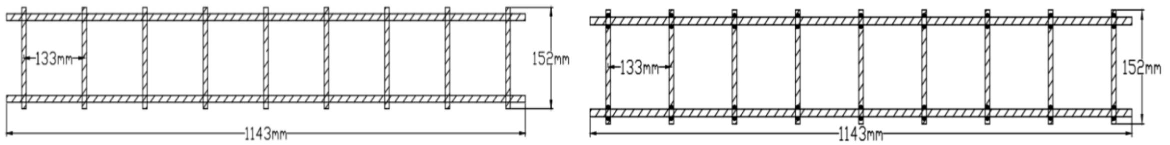

Fig. 2-11 NRSB and WRSB arrangement respectively [4].

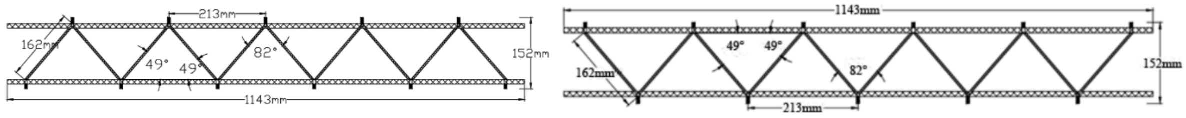

Fig. 2-12 NWWTB and FWWTB arrangement respectively [4].

2.2.2. Validation of Numerical Models with Experimental Data

research by Mohammad Reza Ghasemi and Aydin Shishegaran in 2017**[19]** demonstrated a new approach to increasing the bending strength of simply supported beams by using inclined reinforcement and stress transfer mechanics. Using finite element modeling with ABAQUS software in conjunction with controlled experimental laboratory testing, this paper shows the experimental results closely aligned with numerical solutions and validated that the proposed model is usable as there was good agreement between modeling and physical data**.** Arafa, M., et al in 2018**[5]** examined both the finite element method and experimental results. The comparison between the finite element analysis (FEA) and the experimental test results for the control beam show that the ABAQUS model's predicted failure load is approximately 2% higher than the measured experimental failure load. The FEA's predicted midspan deflection at failure was about 8% lower than what was measured during testing. This indicates that while the numerical model results in an overall slightly higher load capacity, it results in a moderate underestimation of the displacement at failure.

2.3. Design Provisions of shear from Different Codes

The mechanisms responsible for the shear resistance of reinforced concrete members remain Difficult and complex. Different building codes incorporate dissimilar shear design philosophies as a result of various experimental and theoretical bases. Shear failures are particularly unwanted because they are a sudden, unexpected event compared to a flexure failure, which tends to exhibit noticeable deflections before collapse, giving an early warning of possible distress of the structure.

2.3.1. Eurocode 2 (EN 1992-1-1: 2004)

The current European Code EN 1992-1-1: 2004**[28]**, defines the shear resistance of a member with shear reinforcement as the shear resistance provided by the web reinforcements. Shear reinforcement is not required if the resultant shear force is less than the member design shear resistance if there is no shear reinforcement; however, minimum shear reinforcement is needed except in slabs with minor importance and members of minor importance. An empirical equation is provided in the code for the calculation of contribution to shear capacity from the concrete. The empirical equation for concrete contribution accounts for the ratio of longitudinal reinforcement, concrete compressive stress capacity, and presence of axial force. Calculation of the shear force resistance contribution of the transverse reinforcement is based on the variable angle truss analogy. Eurocode doesn't have a specific value for the diagonal crack angle θ, but does provide a recommended limit of $1 < \cot \theta < 2.5$. Conversely, in the same spirit with following the truss analogy, it provides a maximum limit to the shear force to ensure that the diagonal compression force will not exceed the diagonal crushing force of the concrete, V_{fcd} where v is 0.6 for concrete not greater than 60 MPa and 0.9-fck/200>0.5 for concrete grades greater than.

2.3.2. ACI Standard (ACI 318-14)

The ACI sectional shear method, as presented in ACI 318-19**[32]**, is essentially an empirical extension of the 45° truss model. The shear strength equation consists of a concrete contribution, V_c equal to the shear causing the formation of diagonal cracking, and a steel contribution, Vs, that is calculated using the 45° truss equations. In effect, code provisions for determining the shear capacity of structural concrete members with shear reinforcement has been, to a greater or smaller extent, semi-empirically derived, and reference to a truss model has been at best limited. In ACI 318-19, provisions related to the shear capacity of structural concrete members specify the truss model to determine a stirrup contribution to a shear capacity, and then include an empirically determined concrete term.

2.3.3. Canadian Standards (CSA A23.3-14)

CSA A23.3-94**[37]**, the Canadian Standard, offers two approaches for shear strength prediction of reinforced concrete structural components, the Simplified Method and the General Method. The simplified method is similar to the ACI 318 method, with the consideration of member size. The general method relies on the modified compression field theory (MCFT), and therefore shares the same theoretical basis as the AASHTO LRFD method. The Canadian code also suggests the strut-and-tie method for the design of deep beams and other sections of an element that could experience complex variation of strain (D regions).

2.3.3.1. Simplified Method

The simplified approach relies upon the assumption of a 45 degrees truss model. The shear resistance is decomposed to two components, Vc and Vs.

2.3.3.2. General Method

In the general model, the nominal shear strength of a beam is the sum of the concrete contribution, the steel contribution and the effective prestressing force component in the direction of the applied shear.

2.3.4. Japanese Code (JSCE Standard, 2002)

The JSCE code considers three limit states**[33]**: ultimate, serviceability, and fatigue. In terms of design for shear, you must consider the capacities V_{yd} design shear capacity, and V_{wcd} design ultimate diagonal compressive capacity of web concrete.

It is assumed that, after inclined cracking has occurred, the share force is solely carried primarily by the shear reinforcing steel and that the load path is a truss-type mechanism. After that, the members can lose their resistance to shear either by yielding of the shear reinforcing steel which are the tension web chords of the truss or by compressive failure of the web concrete. The component carries by the concrete, V_{cd}, the shear reinforcement, V_{sd}, and the vertical component of the prestress force, V_{ped}.

CHAPTER THREE

3. EXPERIMENTAL PROGRAM

The aim of the experimental program is to assess and compare the shear capacity and failure mode of slender beams with different configurations for the stirrups. The purpose is to investigate load, displacement response and crack development leading to failure of the beams specifically assigned for shear failure. The ambition of the experimental research program is whether or not it is more beneficial to use truss stirrups compared to conventional stirrups, in regards to improving the shear capacity of slender beams.

This research has selected three beam specimens; in order to have a valid and accurate comparison of the influence of stirrup arrangement on shear capacity, it is important to construct all three beams with the same quantity of materials and reinforcement details. Leaning on the same quantity of concrete and rebar per beam is better accomplished if the cross-sectional dimensions, length, and reinforcement ratios are consistent. Thus, this controlled approach establishes the changes attributable solely to stirrup arrangements (conventional vs. truss [non-staggered and staggered]).

Maintaining the materials properties as well as the reinforcement allows the differences in the load carrying and failure modes, and crack patterns to be attributed to the stirrups used and not differences in material strength or amount of reinforcement. This methodology increases the reliability of the comparative study and enhances the overall evaluation of the contribution of truss stirrups to improving the shear resistance of slender beams. The main variable used in this study is the arrangement of stirrup. In this study, a beam with a selected length of 1.75m was used, and shear failure was ensured by using high-strength longitudinal reinforcement bars.

3.1. Materials

The materials used in this study include Cement, River sand, Crushed sand, Coarse aggregate, Water, and Deformed reinforcement bars. The beams in this experimental study were fabricated using concrete and reinforced steel bars. The deformed steel bars were used in the vertical shear stirrups and as horizontal main reinforcement. All the strengths of materials and mechanical properties were measured and discussed in Appendix.

Aggregate

According to BS 882:1992, coarse aggregate includes the larger particles of concrete construction materials, which could be materials retained on the 5 mm sieve. Coarse aggregate also must meet grading and quality requirements as prescribed in the standard **[23].**

The key physical properties of the aggregate such as bulk density, specific gravity, and moisture content were measured and evaluated. The bulk density, specific gravity, and moisture content were all measured and Presented in Appendix.

3.1.1. Concrete Mix-design

The laboratory determined all data necessary for the concrete mix design. The concrete mix was designed with consideration to BS mix design principles. The beams were cast in steel molds and six 150 × 150 × 150 mm concrete cubes were cast to represent the compressive strength of the concrete used. To measure the average compressive strength of the concrete three concrete cubes were tested at 7 days, and a similar test on the remaining three concrete cubes occurred on the day of testing the beam.

Table 3-1 *Concrete mix design*

Mix Design Specifications	
Target Cubic Compressive Strength	30 MPa
Nominal Maximum Aggregate Size	20mm
Cement Type	Ordinary Portland Cement
Amount Required for 1m3 of Concrete Volume	
Lemi OPC Cement	350 Kg
10mm crushed Aggregate	350 Kg
20mm crushed Aggregate	630 Kg
05 mm crushed sand	430 Kg
05mm River sand	480 Kg
fresh Water	165 Kg

3.1.1.1. Compressive Strength Test

According to the BS EN 12390-3 **[24]** standards for hardened concrete, cubical specimens 150 mm in each dimension were prepared and tested for compressive strength. The specimens were surface dried after being removed from the curing tank and ready for testing. Each specimen had a mark identifying each specimen from each mix, measured weight, and were carefully placed under the universal testing machine in Fig. **3-1**. and applied the load by continuous deformation until the specimen failed. Upon failure, it automatically ceased loading and immediately gave an ultimate load and compressive stress reading on the display which was also recorded. Six cube samples were prepared for testing, and three of these were tested at seven days and the remaining three on the time of the beam test.

Fig. 3-1 *Compressive strength test of concrete*

Table 3-2 *Compressive strength result*

Sample	**Days**	**Failure Load (kN)**	**Weight(gm)**	**Compressive Stress (MPa)**	**Average cubic stress (MPa)**
1	7	492	8,505	22	21
2	7	470	8,463	21	
3	7	471	8,430	21	
4	28	687	8,522	31	30
5	28	678	8,431	30	
6	28	664	8,454	30	

3.1.2. Reinforcement

In all specimens a 20mm, 14mm and 10mm diameter deformed reinforcement was used as longitudinal bar while deformed 8mm diameters were used as transverse reinforcements. Uniaxial tensile tests were performed on rebar samples from the different diameters used. The overall laboratory physical examination of rebar is provided in Appendix.

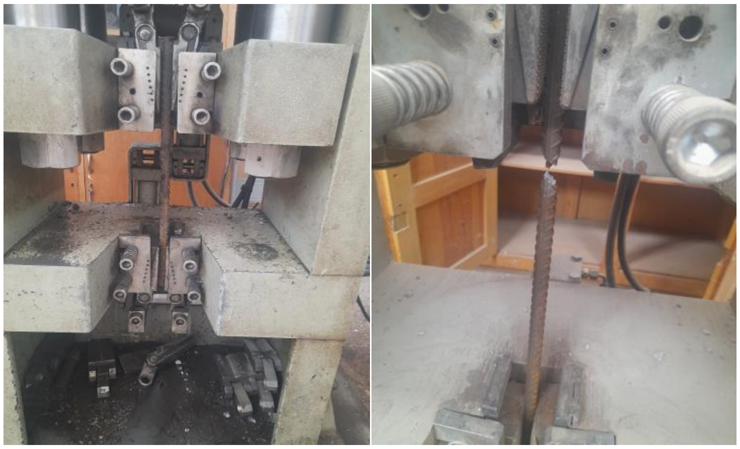

Fig. 3-2 *Uniaxial tensile tests of rebar*

3.1.3. Specimen Production

The process of manufacturing specimens can be broken down into three phases: preparation and assembly of formworks, fabrication of reinforcement cages and placement of rebar cages within the formworks after placing the essential accessories. Specimen preparation is completed by pouring the concrete in the prepared formworks.

Slender reinforced concrete (RC) beams are structural elements defined by high shear span-to-depth (a/d). Kani **[31]** and ACI 318 **[32]** have defined slender beams as beams which have an a/d of greater than 2.5; JSCE **[33]** has defined slender beams as having an a/d greater than 2; Eurocode 2 (EC2) **[34]** has defined slender beams as those having an a/h of greater than 3.

According to our design intention, the beam is designed as a slender beam and a ratio of shear span to effective depth is 3.11, confirming that it is slender since it is greater than 2.5.

Table 3-3 *Dimensions of beam specimens*

specimen	Height (mm)	Width (mm)	concrete cover (mm)	Effective depth (mm)	Shear span (mm)	a/d	spacing (mm)	Weight (kg)
CB	260	170	25	217	675	3.11	200	14.93
TBNS	260	170	25	217	675	3.11	270	14.92
TBS	260	170	25	217	675	3.11	270	14.95

3.1.4. Formwork

In general, plastic plywood refers to wood-plastic composites (WPC) boards where wood fibers or veneers are mixed with plastic resins (for example polyethylene, polypropylene, or PVC).

Fig. 3-3 *Wood-plastic composite formwork*

3.1.5. Reinforcing cages

Reinforcing cages are components made of steel reinforcement bars that are shaped and tied together in such a way as to create a cage to be inserted inside a concrete element such as a wall, column, beam, slab or pier. Reinforcing cages are needed to provide the tensile strength and stiffness needed to provide durability to reinforced the concrete structure.

Fig. 3-4 *Conventional beam reinforcement cage*

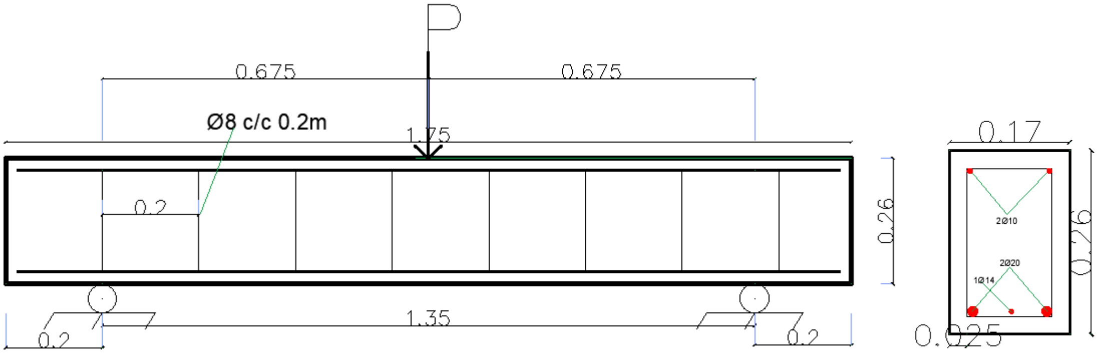

Fig. 3-5 *Profile and details of conventional beam*

Fig. 3-6 *Non-staggered truss reinforcement cage*

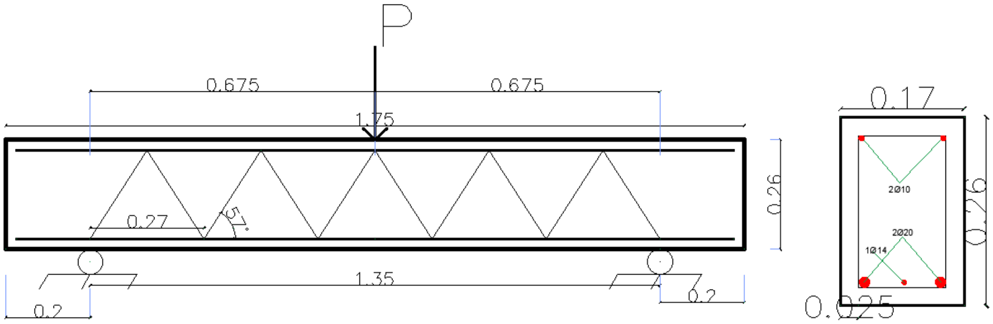

Fig. 3-7 *Profile and details of non-staggered truss beam*

NB: Units are in meter

Fig. 3-8 Staggered truss reinforcement cage

3.1.6. Concrete spacers

Concrete spacers uniformly hold the rebar cage in place and prevent downward motion during the pouring of the concrete, which enhances construction quality and helps prevent honeycombing or voids in concrete around the rebar. The spacers were prepared as follow.

Fig. 3-9 *Spacers*

Upon completing the preparation of the rebar and formwork, concrete spacers are placed. After the spacers are installed, the reinforcement cage was set in the proper location within the provided formwork.

Fig. 3-10 *Reinforcement cages set in to formwork*

3.1.7. Casting concrete

Casting concrete is the placement and shaping of concrete in formwork to form objects and or structural elements, followed by the curing process, where concrete gains strength. After casting, the formwork was removed after 48 hours and concrete was moist cured for 14 days.

Fig. 3-11 *Beam Concrete Casting*

Fig. 3-12 *Beam specimens after dismantling formwork*

3.2. Test Setup and Instrumentation

The experimental program involved the testing of Three shear critical slender reinforced concrete beams in a three-point monotonic loading system. The beams were simply supported on two steel roller supports on each side. A concentrated load was applied using a hydraulic jack that has a maximum capacity of 300 kN.

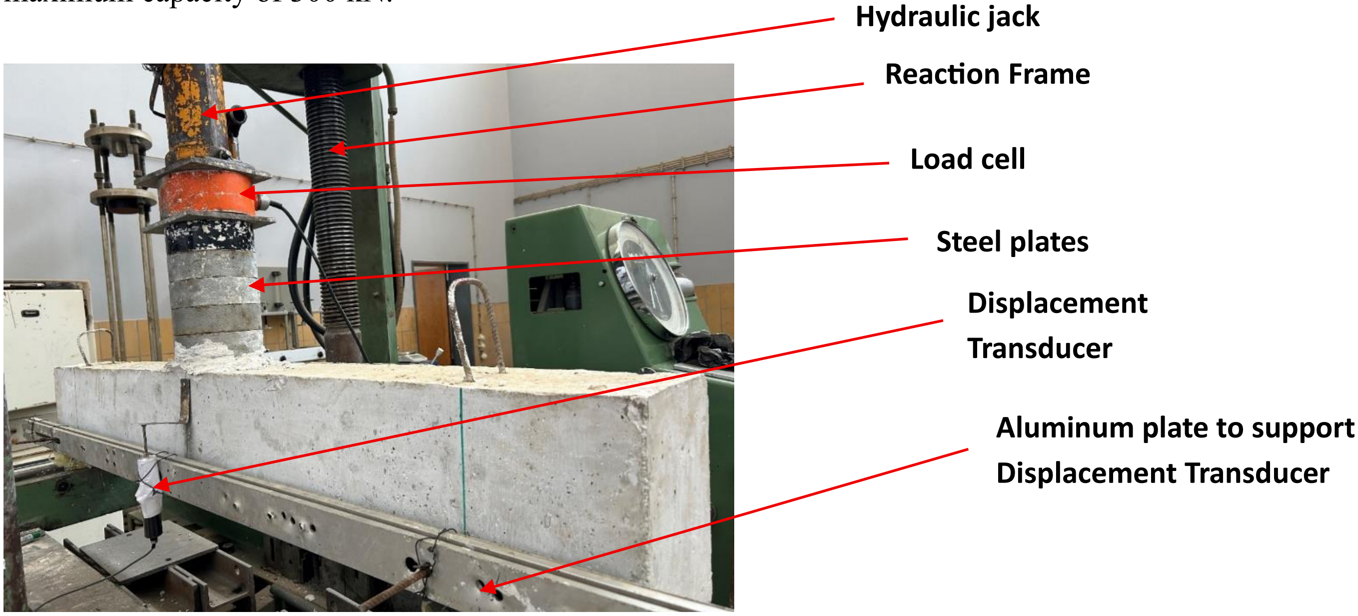

Fig. 3-13 *test set up*

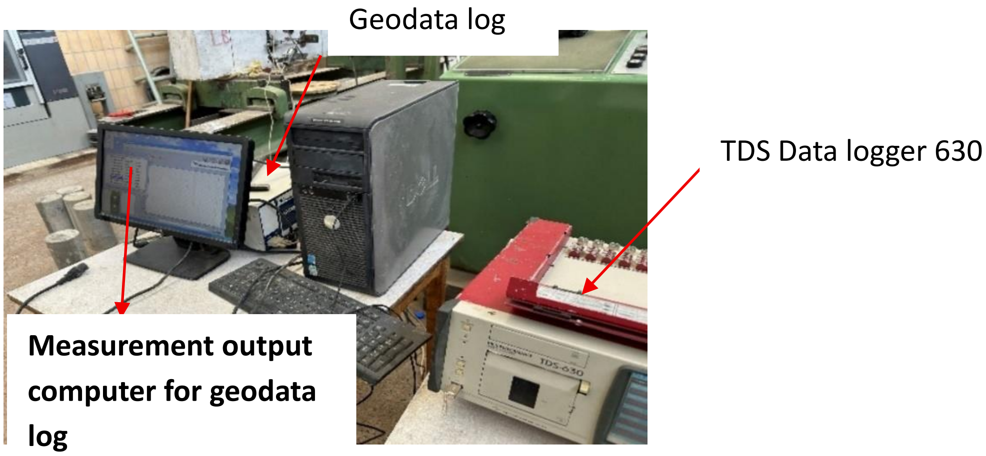

Fig. 3-14 *Data collector and output*

3.2.1. Surface Mounted Displacement Measurement

A surface displacement measurement system was installed on the left-hand side of the front face of the beam. The system included two diagonal sensors installed at 45° and 135°, respectively, and one horizontal sensor and the gage lengths are 17cm. Each specimen was outfitted with a total of three LVDTs for the measurement of surface displacement.**[39]**

To track shear strain, we use transducers as shown in Fig. **3-15**. The surface monitoring system tracked shear strain at the front of each beam. The left side of front surface measurements were taken over a 12 cm by 12 cm area with the 17 cm gage. Displacement measurements from both LVDTs were obtained from the Geodata log system using one second intervals with readings in millimeters. The strain was calculated by dividing the measured change in length by the overall length of 17 cm. Negative strain indicates compression and positive strain tension.

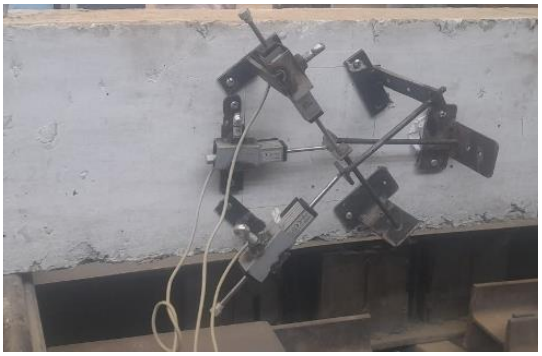

Fig. 3-15 *Transducers attached on beam surface*

CHAPTER FOUR

4. NON-LINEAR FINITE ELEMENT ANALYSIS

4.1. Finite element modeling

Finite element modeling is an excellent method to accurately model the behavior of reinforced concrete structures that cannot be modeled through experiment and support a number of loading conditions including static, dynamic, cyclic, seismic, thermal, and live and boundary conditions. FEM provides many beneficial aspects, including, but not limited to: accuracy, efficiency, versatility, visualization, and verification. In the present study FEM used to verify experimental work and to identify the best inclination angle. A 3D nonlinear finite element model was created to study the shear behavior of RC beams with the commercial package, Abaqus 2020. As one of the available Finite Element Analysis (FEA) software packages, it is well known and has been widely used in the field of civil engineering. The beams being modeled for FE analysis, had the same property as to those in the respective experimental specimens, confirmed through earlier work. This research has been used five models three of them are the same as the experimental model the other two are with 45^0 Inclination.

4.1.1. Geometry model

4.1.1.1. Concrete model

The concrete part was analyzed with eight-node linear brick elements with a reduced integration point (C3D8R). The shape function for this element is the same as the eight-node full integration brick element (C3D8).

The C3D8 is a linear brick (hexahedral) element with 8 nodes and full integration. The term "full integration" means that it has 8 integration points (2x2x2) inside the element for numerical integration. Therefore, it is a more accurate element, but it can be affected by "locking" conditions, particularly in bending situations. Additionally, it requires more computational effort because it uses full integration.

The C3D8R is also an 8-node linear brick element, but it utilizes reduced integration, only having 1 integration point. The C3D8R element also has hourglass control in order to mitigate zero-energy modes (hourglass modes). The C3D8R element is computationally efficient compared to C3D8, and it still experiences some locking behavior.

Here are important characteristics of the C3D8R element: -

- The element is an 8-node linear brick solid element with reduced integration using only 1 integration point, which promotes computational efficiency, and reduces locking phenomena (shear locking, volumetric locking) that may occur in fully-integrated elements.
- Because of reduced integration, it can have hourglass (zero-energy) modes, so hourglass control is implemented to stabilize the element to avoid non-physical deformation patterns.
- It does not have volumetric locking like fully integrated elements, but is more sensitive to shear locking than various advanced element types.

4.1.1.2. Reinforcing steel model

The reinforcement was modeled as T3D2 elements which are linear truss elements. The reinforcement cage was connected to the concrete using the embedded region constraint in Abaqus.

4.1.2. Material model

4.1.2.1. Concrete

The material constitutive behavior of concrete is non-linear and complex by nature; however, finite element packages can replicate these complex behaviors. ABAQUS has the ability to simulate damage using any of the three different crack models for RC elements: (1) smeared crack concrete model, (2) brittle crack concrete model, or (3) concrete damaged plasticity models. All three models can apply to concrete with reinforcement. The CDP model was used in this study because it can simulate the complete inelastic behavior of concrete throughout its range of tension and compression, including the damage characteristics. It has a general capability to model concrete and other quasi-brittle materials in all types of structures. The concrete damaged plasticity model combines isotropic damage elasticity with isotropic tensile and compressive plasticity to simulate the inelastic behavior of concrete. The CDP model recognizes tensile cracking and compressive crushing both as failure modes for concrete. The uniaxial tensile and compressive relationships are determined by the damaged plasticity in the model.

4.1.2.2. Numerical model for compressive behavior of concrete

In a concrete damage plasticity model, the plastic hardening strain in compression $\varepsilon^{pl}{}_{,c}$ was critical in establishing the relationship between the damage parameters and the compressive strength of concrete as shown in Fig. 4-1& 4-2[**26].**

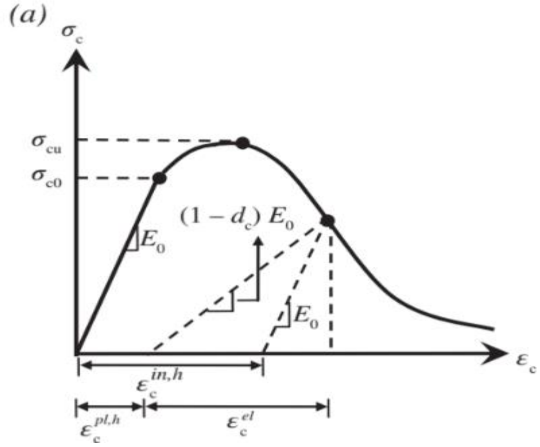

Fig. 4-1 *Response of concrete to a uniaxial loading condition, compression [31].*

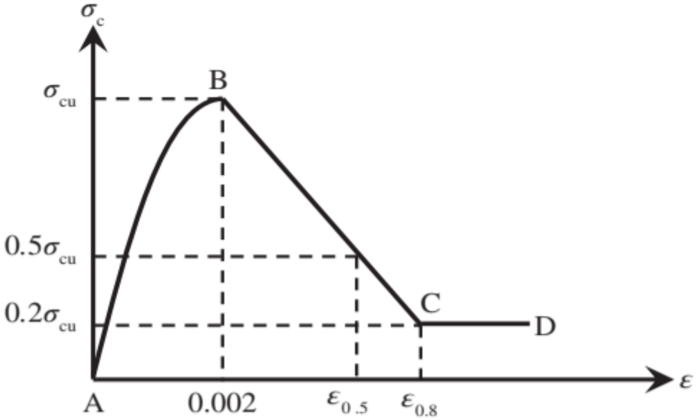

Fig. 4-2 *Kent and park model for confined and unconfined concrete [30].*

$$\varepsilon_c^{in} = \varepsilon_c - \varepsilon_{0c}^{el} \qquad (1)$$

Where, $\varepsilon_{0c}^{el} = \frac{\sigma c}{E_0}$, is the elastic strain corresponding to undamaged material and ε_c is the total strain.

Abaqus converts the inelastic strain, ε_c^{in} to plastic strain ε_c^{pl} by using Eq. (2).

$$\varepsilon_c^{pl} = \varepsilon_c^{in} - \frac{d_c}{(1-d_c)}\frac{\sigma_c}{E_0} \qquad (2)$$

Where, dc is the concrete compressive damage parameter.

Generally, the uniaxial compressive behavior can be described by either experimental tests or existing constitutive models that are based on the unconfined concrete (e.g. Hognestad and Kent et al.). However, the current study has used the Kent and Park parabolic constitutive model for unconfined concrete, which can be written as follows:

$$\sigma_c = \sigma_{cu} \cdot \left[2\left(\frac{\varepsilon_c}{\varepsilon_c'}\right) - \left(\frac{\varepsilon_c}{\varepsilon_c'}\right)^2\right] \qquad (3)$$

Where:

- σ_c = stress in the concrete
- σ_{cu} = ultimate compressive strength of concrete
- ε_c = strain in the concrete
- ε_c' = strain at peak compressive strength

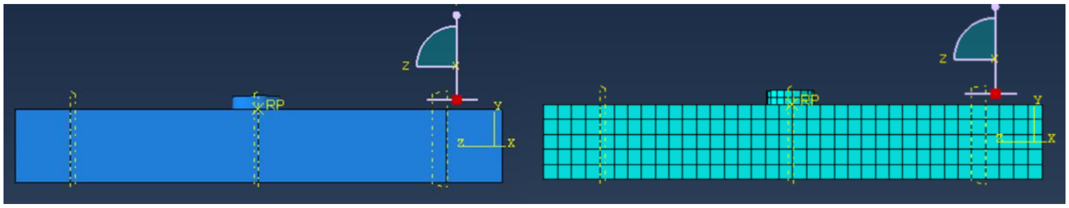

Fig. 4-3 *FEM model of beam and mesh respectively*

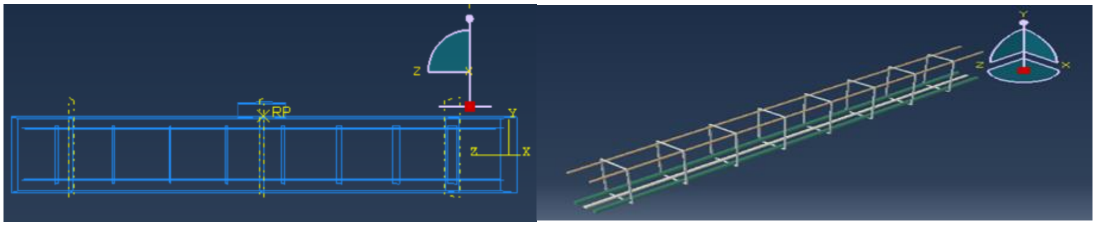

Fig. 4-4 *FEM model of assemble body and Reinforcement cage of CB(90^0) Respectively*

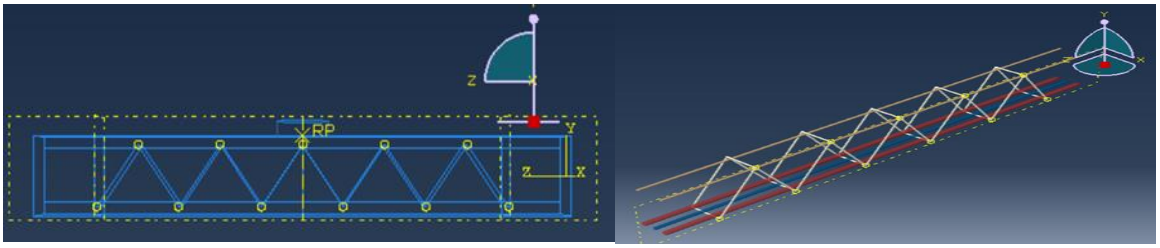

Fig. 4-5 *FEM model of assemble body and Reinforcement cage of TBNS(57^0) Respectively*

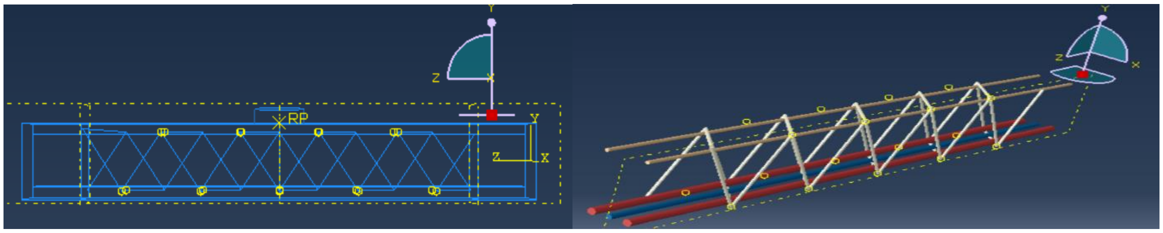

Fig. 4-6 *FEM model of assemble body and Reinforcement cage of TBS(57^0) Respectively*

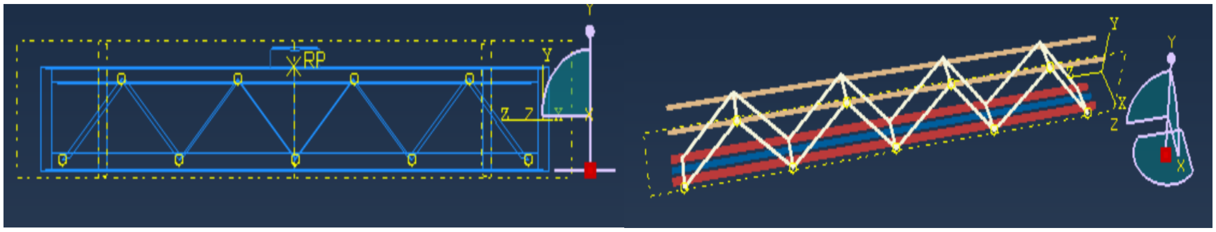

Fig. 4-7 *FEM model of assemble body and Reinforcement cage of TBNS(45^0) Respectively*

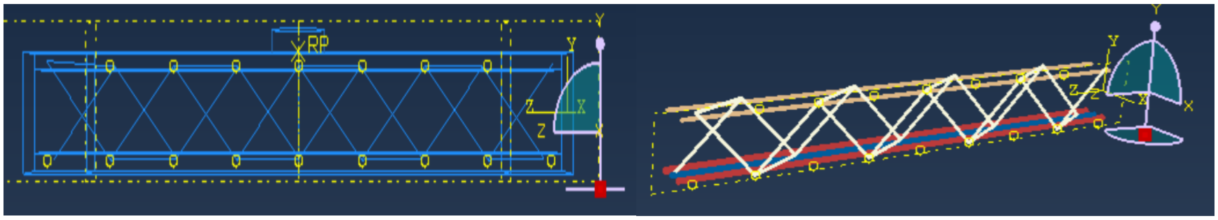

Fig. 4-8 *FEM model of assemble body and Reinforcement cage of TBS(45^0) Respectively*

4.1.2.3. Numerical model for tensile behavior of concrete

The finite element method (FEM) was used for numerical non-linear analysis to assess the tensile contribution of concrete after reinforced concrete beams develop flexural cracking **[27].**

$$f_{ct\ max} = 0.7*\sqrt{fck} \qquad (4)$$

$$\varepsilon_{cr} = \frac{fct\ max}{E_{cm}} \qquad (5)$$

where $\mathbf{f_{ct\ max}}$ Concrete tensile stress

ε_{cr} Concrete tensile strain

$\boldsymbol{E_{cm}}$ Modulus of Elasticity

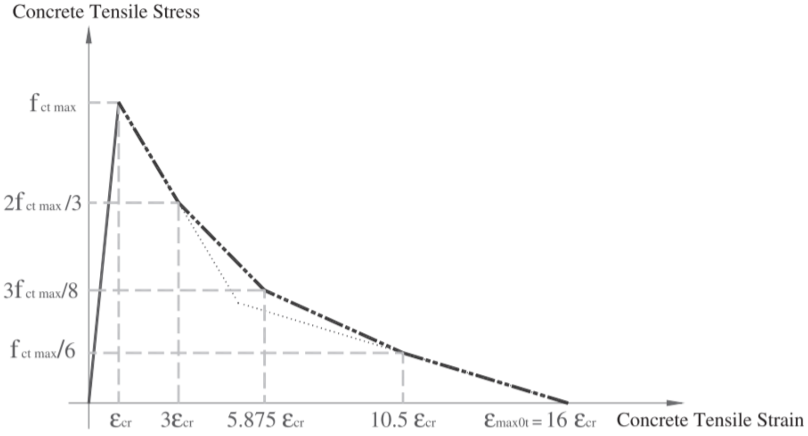

Fig. 4-9 *Tension Softening Curve [27]*

4.1.3. Mesh

Ultimately, the mesh sizes are also important in a numerical simulation. The mesh represents the corresponding structural and material properties of the structure in question and greatly relates to the resulting responses based on the requested loads applied. Strain localization in finite element modeling affects only some sections of the structure, allowing the rest of the structure to be unloaded, and therefore indicating that the numerical model also relies on mesh size. The finer the grid (or mesh), the more precise the result will be. The effects of increasing fineness are that more time is spent in calculation (more complex calculations). The ideal situation in finite element method means that it will converge given sufficient line refinement has been carried out to reach a reasonable convergence point. The mesh size in this study was 50mm and 40mm for concrete and reinforcement respectively.

4.1.4. Interaction

In this paper truss elements were used to model reinforcement which was embedded in the host continuum solid elements. Embedded, in this context, means that the translation degree of freedom at the nodes of the embedded element are removed, and constrained to the corresponding interpolated value in the host continuum element. To eliminate stress concentrations in the concrete beam, the reaction forces are transferred to the beam through plates defined as discrete rigid bodies. The plate transferring the reactions from the supports are connected to the beam specimen using the “tie” option, which cannot be disconnected during loading.

4.1.5. Boundary conditions

The beams were simply supported and had a clear distance of 1.35 m between the supports. The beam was restrained on both side of the support in y direction only (roller support model). The plate at mid span was initially restrained in the x and y-direction and the load is applied through rigid body mechanism.

4.1.6. Dilation Angle

When an element deforms as a result of applied stress, its angle is called the dilation angle (Ψ) and it quantifies the volumetric change that occurs in a concrete particle when it undergoes shear deformation. Its value is usually in the range of (25-50) degrees based on what previous researches had used. The volumetric strain from plastic deformations depends on the dilation angle**[25]**, 45° was chosen since it had the best fit to the experimental curve.

4.1.7. Viscosity

In ABAQUS/Standard, the concrete damaged plasticity (CDP) model has a viscosity regularization parameter. The CDP model considers degradation of elastic stiffness due to plastic straining in compression or tension, and is based upon isotropic damage.

This study applies viscosity to calibrate the duration of the analysis. Therefore, given better correlation with the experimental data, the selected viscosity value is μ=0.00001 for all samples in this study.

4.1.8. Shape factor

In the ABAQUS concrete damaged plasticity model, the yield surface shape is determined by shape factor Kc which is used to quantify mesh efficiency. Only tetrahedral and triangular elements have indices for the shape factor. The shape factor description is a number between 0 and 1 where 0 is a degenerate element and 1 is the ideal element shape. The value of Kc was defined from a range that had been established from a study of several other authors who conducted FE studies of concrete structures. For this research, Kc=0.667 was used because it provided the best curve fitted with the experimental curve.

4.1.9. Damage plasticity model

In ABAQUS, accurate description of concrete strength with triaxial stress requires the complete description of five parameters to fully characterize plastic behavior. The five parameters are: the dilation angle (ψ), eccentricity (ε), the ratio of the biaxial yield compressive stress and uniaxial yield compressive stress, the parameter (Kc), and the viscosity parameter. The preferred recommendations for these parameters in ABAQUS are shown in Table 4.1.

Table 4-1 *CDP parameter for all beams*

Dilation angle (ψ)	**Eccentricity (ε)**	f_{bo}/f_{co}	K_c	**Viscosity parameter**
45^0	0.1	1.16	0.667	1.00E-05

4.2. Loading and Interpretation of Results

Displacement controlled load was applied to obtain the post-peak response of the reinforced concrete beams following depth criteria. The Displacement was applied to the beam in a time step loading. As a result, the nonlinear finite element software shows respective responses of each increment.

CHAPTER FIVE

5. RESULT AND DISCUSSION

5.1. Result from experiment

In this section the Experimental results of the beams are presented and discussed. In all three specimens, typical shear failure occurred. First, small flexural cracks formed at the bottom of the mid span. After some time, diagonal cracks formed and continued to widen until the beams eventually failed. With reinforced concrete beam, the reinforcement steel goes to the yield strength of the steel before the concrete reaches its maximum stress capacity. As the steel yields cracks will begin to form in the beam. The specimens failed when it showed large displacements along with negligible increase in load. The ultimate load was taken as the maximum load reached. The load from hydraulic jack was applied at an Average rate of 0.45 kN/s - 0.5 kN/s for all beam.

5.1.1. Control Beam (CB)

The Control Beam (CB) failed in shear failure Mode. At first, very thin flexural cracks developed at the bottom of the midspan. Then after a period of time, diagonal cracking emerged on left side of front face of beam (right side of back face), also there is diagonal crack on right side of front side, but the dominant diagonal crack shows on the left side of front face as shown fig. **5-3** below when the beam was near the shear span, with cracking becoming larger in width until failure. Its ultimate load capacity was the lowest for all three specimens, demonstrating the level of shear resistance without any particular longitudinal stirrup arrangements. As the load increased, failure mode changed from flexural to shear, and the beam failed with a maximum ultimate load of 210.65 kN.

Fig. 5-1 *Back and Front side of CB specimens Before failure Respectively*

Fig. 5-2 *Back and Front side of CB specimens After failure Respectively*

Fig. 5-3 *Left Front side of CB specimens After failure*

Fig. 5-4 *Right Front side of CB specimens After failure*

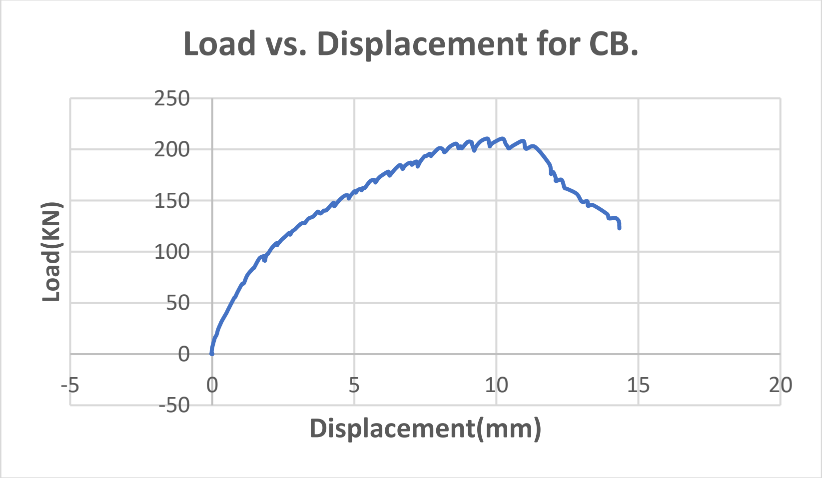

Fig. 5-5 *Load vs. mid-span deflection curve of CB*

5.1.2. Truss Beam Non-Staggered (TBNS with 57^0 inclined)

The TBNS specimen exhibited the same cracking sequence as the CB, flexural cracks at midspan, then diagonal cracking, however, diagonal cracks appeared both sides, but the dominant was at right side of front face of beam (left side of back face) at higher loads than in the CB, thereby the shear resistance achieved a higher load due to the stirrup was in a non-staggered truss position. The failure mode remained as wave yielding and rupture of web reinforcements. The TBNS beam had a higher ultimate load capacity than the CB due to the non-staggered truss stirrup arrangement and better shear resistance. The ultimate shear failure happened at 249 kN. Therefore, it can be stated that the non-staggered truss beam had more load capacity than the conventional beam.

Fig. 5-6 *Back and Front side of TBNS specimens Before failure Respectively*

Fig. 5-7 *Back and Front side of TBNS specimens After failure Respectively*

Fig. 5-8 *Left Front side of TBNS specimens After failure*

Fig. 5-9 *Right Front side of TBNS specimens After failure*

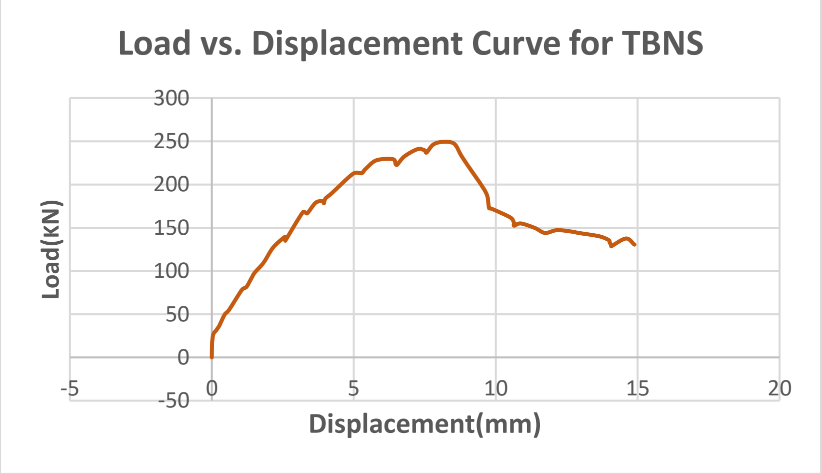

Fig. 5-10 *Load vs. Mid-span deflection curve of TBNS*

5.1.3. Truss Beam Staggered (TBS with 57^0 inclined)

In the TBS specimen, the crack formation mechanism was the same as the previous two beams, the TBS specimen exhibited the highest load capacity of all the specimens indicating that configuration has the max contributions for enhanced shear strength through shear stirrup density. Diagonal cracks appeared both sides, but the dominant was at right side of front face of beam (left side of back face). As the load increased the failure behavior transitioned from flexural to shear behavior. The ultimate shear failure happened at 267.01 kN. the staggered truss beam supported a higher ultimate load than both the conventional and non-staggered truss configurations.

***Fig.** 5-11 Back and Front side of TBS specimens Before failure Respectively*

***Fig.** 5-12 Back and Front side of TBS specimens After failure Respectively*

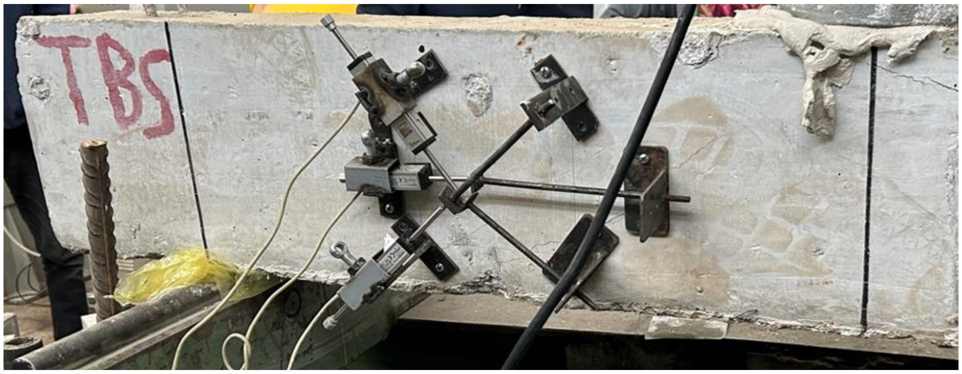

***Fig. 5-13** Left Front side of TBS specimens After failure*

Fig. 5-14 *Right Front side of TBS specimens After failure*

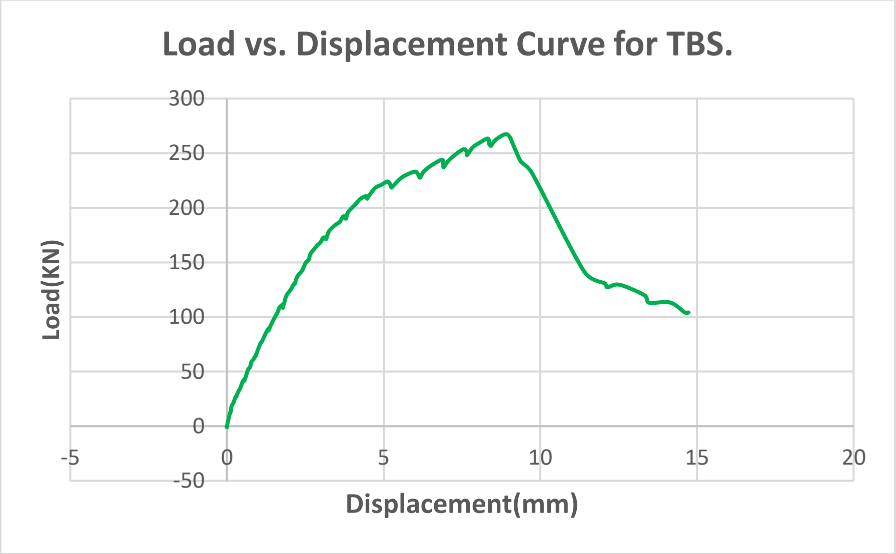

Fig. 5-15 *Load vs. mid-span deflection curve of TBS*

5.1.4. Comparison of Experimental Results

The three beams exhibited different stirrup arrangements that had a significant effect yielding different shear strengths in the following order: CB < TBNS (57^0) < TBS (57^0)

The non-staggered truss beam has an ultimate load capacity that is around 18.25% higher than a conventional beam, while the staggered truss beam has an ultimate load capacity that is around 26.75% higher than a traditional beam. These observations mean both truss beam configurations improve shear load capacity capabilities over the traditional beam, with the staggered configuration having the enhanced shear load capacity over the non-staggered configuration. The formation of crack in TBNS and TBS were relatively slower than CB. Upon observing the deflection at the yield load, TBS and TBNS has less deflection than CB, regardless of CB producing less yield load than TBNS and TBS. Therefore, beam TBNS and TBS had more strength and stiffness than CB.

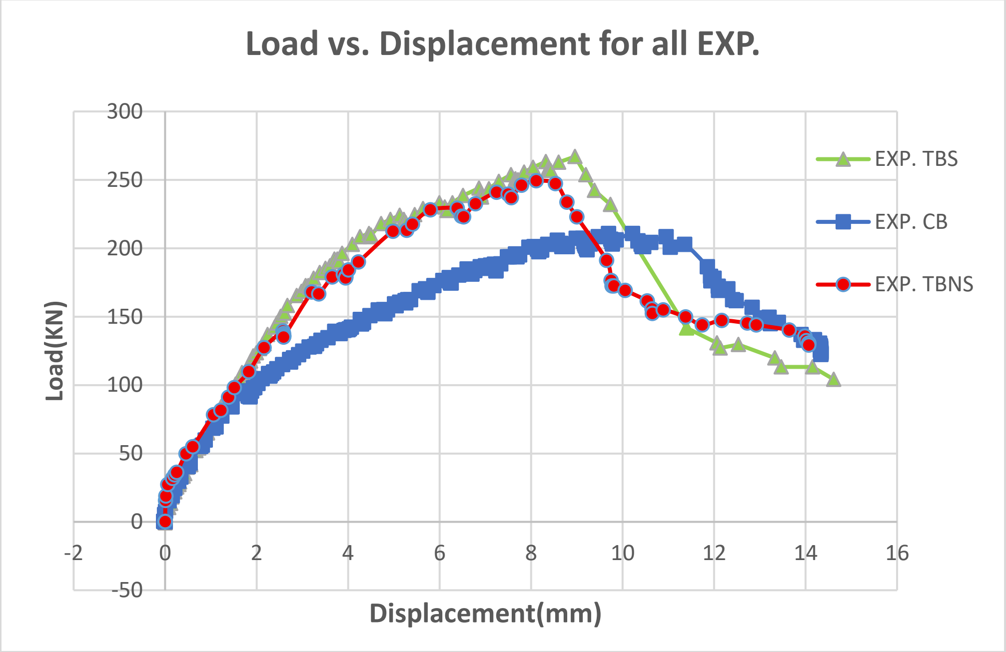

Fig. 5-16 *Load vs. mid-span deflection curve of all experimental beams*

Where EXP. CB ……. experimental result of control beam

EXP. TBNS … experimental result of Truss beam non-staggered

EXP. TBS ...… experimental result of Truss beam staggered

5.1.5. Comparison of Results with Existing Literature Review

The present study shows an 18.25% increase in shear capacity with a non-staggered arrangement (57^0). This is compared to previous studies that utilized inclined and truss stirrup arrangements, as summarized below. Aminuddin Bin Suhaimi (2015) used inclined shear reinforcement as stirrups and reported an 18% to 33% increase in beam shear capacity, which aligns well with the present study. Zamri and Mohammed (2018) observed a 20.8% increase using an inclined stirrup arrangement. Nasra and Asha (2013) reported a 35% increase in shear capacity with inclined stirrups, while Mahzuz (2021) found a 34% increase using a truss stirrup arrangement.

As observed from the existing literature, some results exceed the 18.25% increase found in this study. This discrepancy can be attributed to differences in the a/d ratio, where the previous studies used values less than 2, whereas the present study has an a/d ratio greater than 2. Since an increasing a/d ratio reduces shear capacity, the higher percentages reported in the literature compared to the present study are consistent with this trend.

5.2. Finite Element Method (FEM) Results

In this section the FEM results of the beams are presented and discussed. This study utilizes the Finite Element Method (FEM) to carefully validate experimental work by modeling the physical behavior that seen in experiments to confirm that this research uses the same FEM simulation as what was experimentally observed. This study is replicating the experimental results with the FEM analysis, which shows a good match to observed physical data (e.g. crack initiation, crack propagation, shear capacity), allowing to have confidence in the reliability and validity of the experimental data. This process gives more overall confidence because it reaffirms all the conclusions, as well as validates the overall experimental methodology. For each beam the study tries to extract five characteristics from the visualization that shows the model result with the help of image those are express as follow:

5.2.1. DamageC

DamageC in Abaqus generally refers to damage variable related to damage mechanics that displays the level of damage initiation or evolution within the material, typically with regard to cracks or fractures. It indicates areas in the model where damage initiates or accumulates.

5.2.2. DamageT

DamageT in Abaqus corresponds with damage in tension, or damage degradation due to tensile loading conditions. DamageT shows the regions in the model where the tensile damage has an effect, often meaning that material damage is present, and ultimately could lead to material failure.

5.2.3. U,magnitude

U,magnitude in Abaqus visualization refers to the magnitude of (usually nodal) displacement. U,magnitude indicates how far points in the model have moved from their original position as a result of any applied loads or boundary conditions that dictate those points' position.

5.2.4. PEEQ

PEEQ is short for "Equivalent Plastic Strain," which is a measure of the material's irreversible accumulated plastic deformation. PEEQ will indicate how much permanent deformation the material has gone through, and is important for characterizing failure or yielding for materials of interest.

5.2.5. S Mises

S Mises (Von Mises stress) is a scalar stress value used to predict yielding of ductile materials under complex loading. Von Mises stress condenses all principal stress components into equivalent stress density value which can be used to compare to the yield strength of the material. It is used to pull-out aspects that indicate potential failure zones.

5.2.6. FEM Analysis of Control Beam (CB)

The FEM model of the CB was able to Simulate the experimental mechanism of crack initiation and crack development, a behavior that began with flexural cracks and transitioned to shear diagonal cracks. The FEM-predicted ultimate load was congruent with the experimental value, justifying the simulation for the control specimen. The failure was Shear failure at ultimate load of 187.45kN

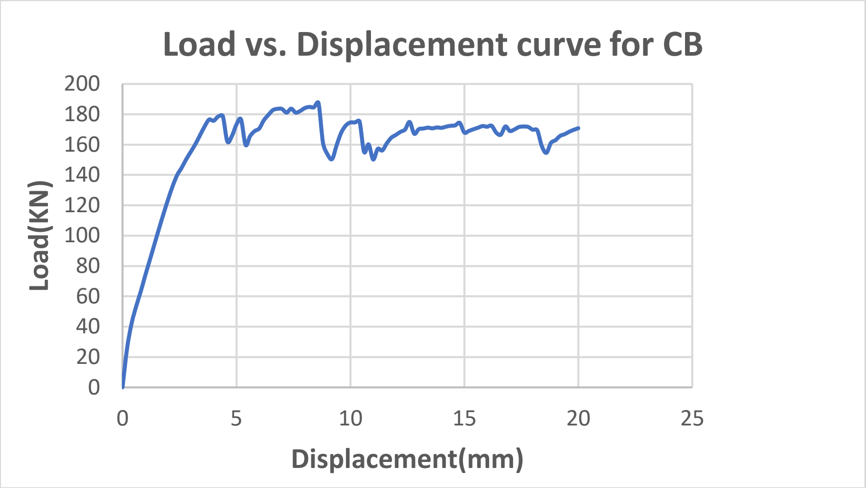

Fig. 5-17 *Load vs. mid-span deflection curve of FEM CB*

The fig. **5.18** as shown below shows that the left side of front beam is more damage as like Experimental result.

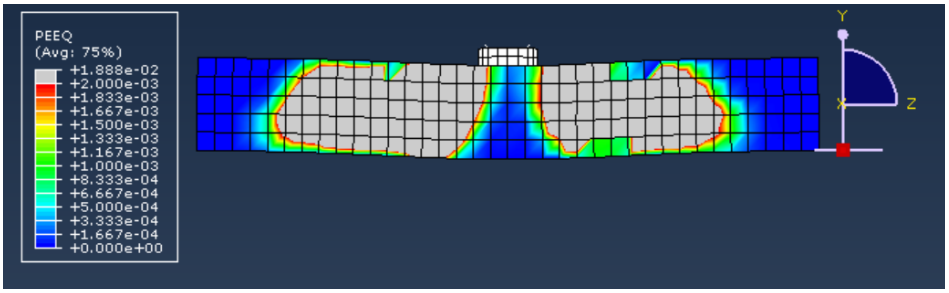

Fig. 5-18 *Equivalent Plastic Strain of CB*

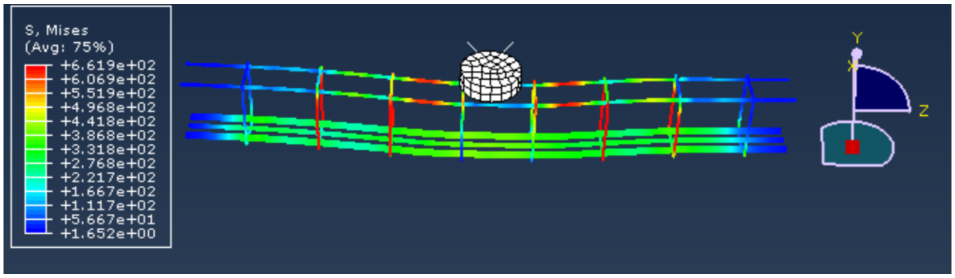

Fig. 5-19 *Von Mises stress of CB*

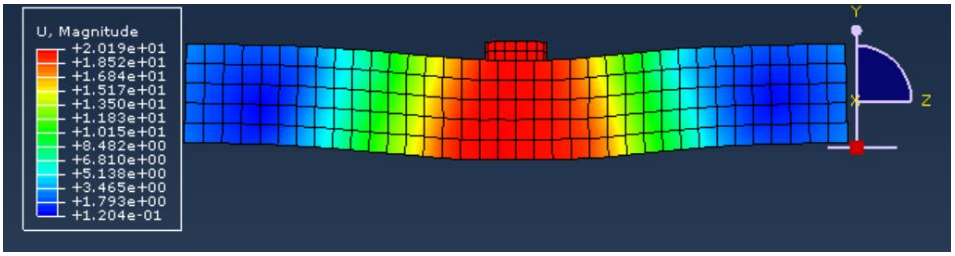

Fig. 5-20 *U, magnitude of CB*

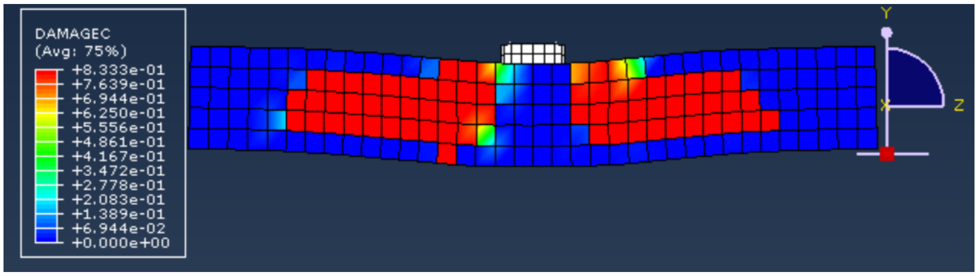

Fig. 5-21 *DAMAGEC of CB*

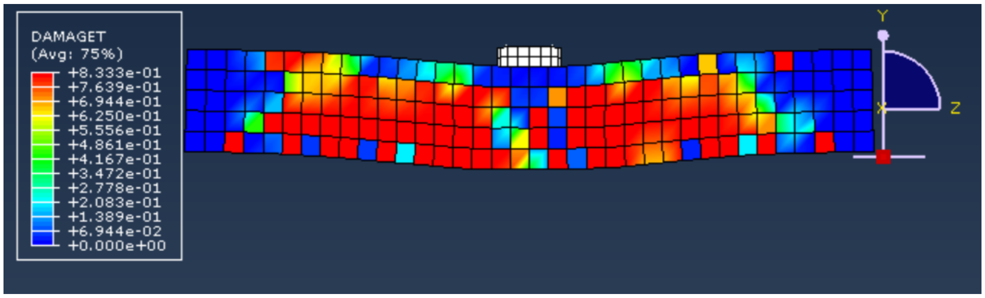

Fig. 5-22 *DAMEGET of CB*

5.2.7. FEM Analysis of Truss Beam Non-Staggered (TBNS with 57^0 inclined)

From the TBNS beam, the FEM modelling noted a higher shear capacity, with a pattern of cracking and failure mode somewhat similar to the experiment. The results from the FEM model indicate a greater ultimate load capacity of the model than what was observed in the FEM CB. It appears that the non-staggered stirrups delayed the formation of diagonal cracks. The beam was failed in shear at ultimate load of 245.74kN.

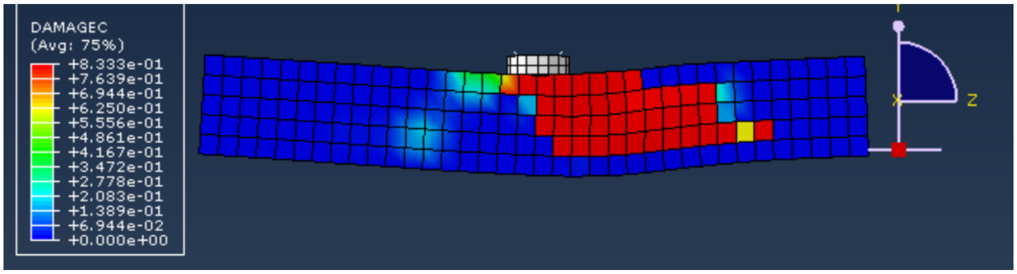

Fig. 5-23 *DAMAGEC of TBNS*

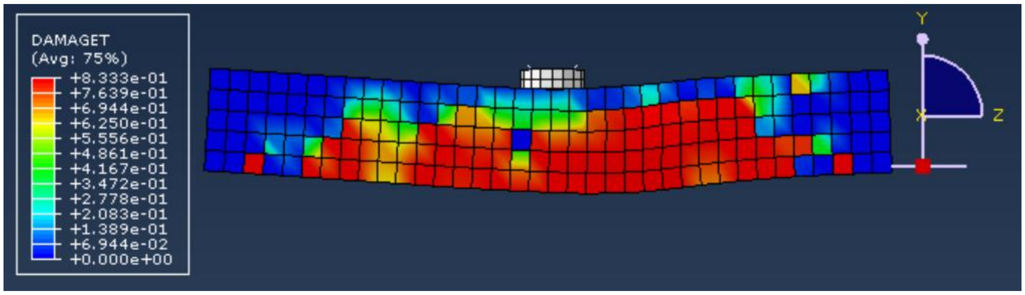

Fig. 5-24 *DAMEGET of TBNS*

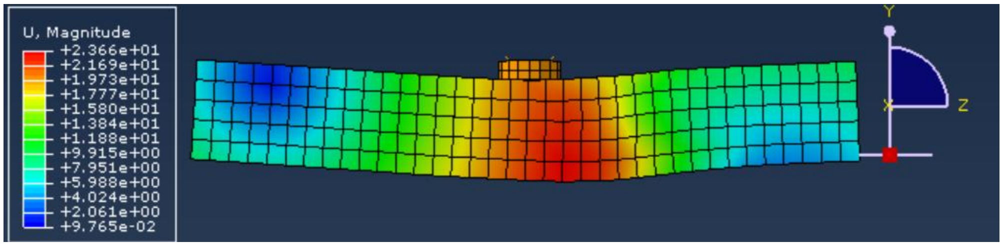

Fig. 5-25 *U, magnitude of TBNS*

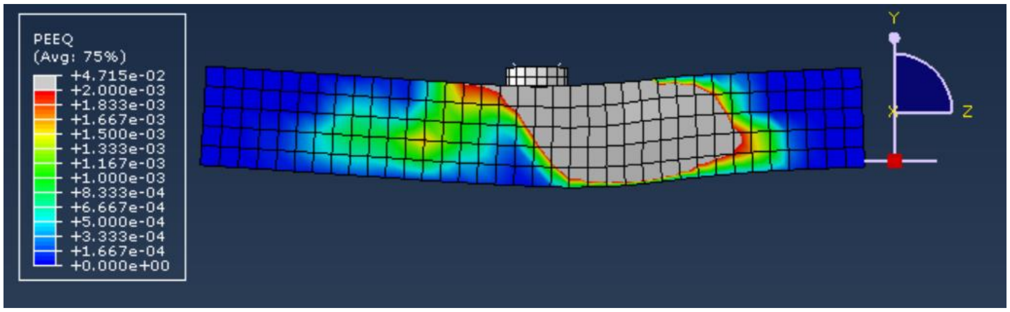

Fig. 5-26 *Equivalent Plastic Strain of TBNS*

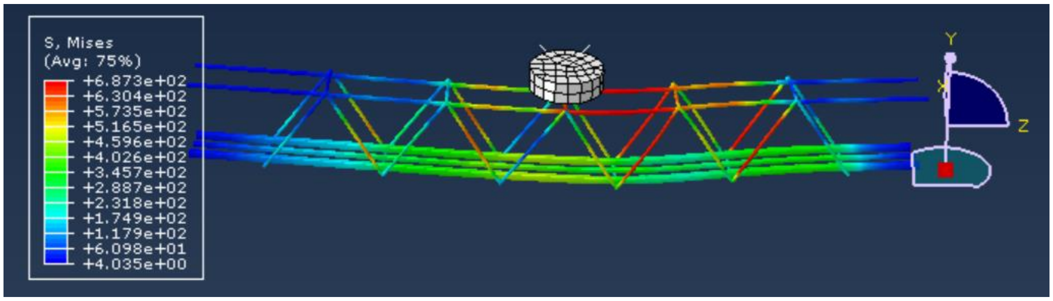

Fig. 5-27 *Von Mises stress of TBNS*

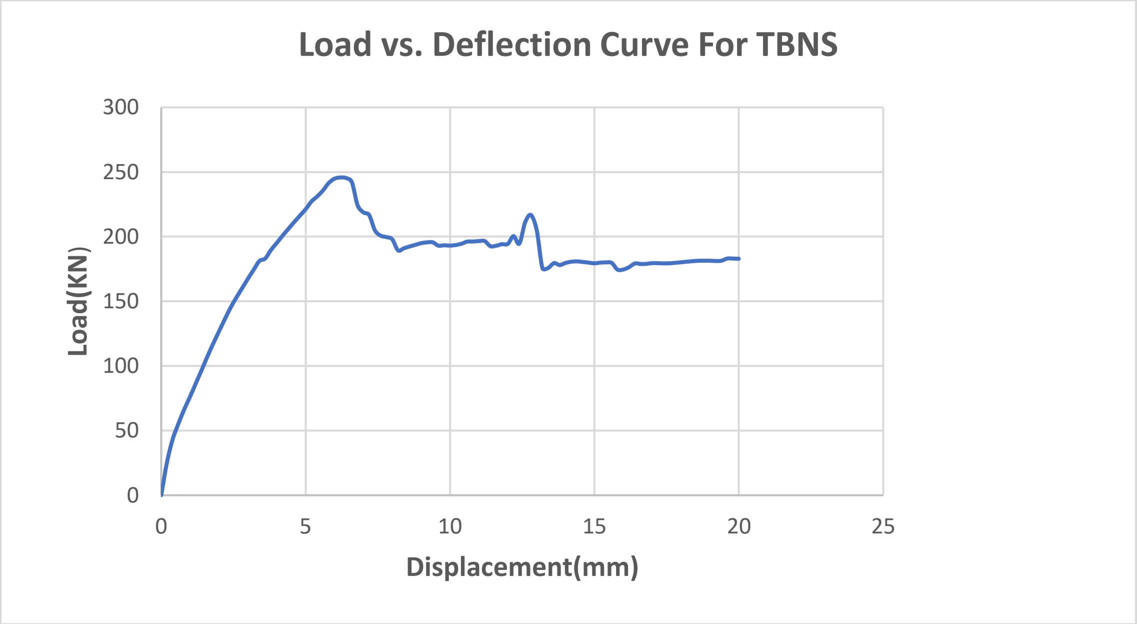

Fig. 5-28 *Load vs. mid-span deflection curve of FEM TBNS*

5.2.8. FEM Analysis of Truss Beam Staggered (TBS with 57^0 inclined)

The staggered stirrup arrangement in the FEM model provided better confinement of the concrete in the model and as a result delayed crack propagation, and increased the ultimate capacity of the beam. The projected load carrying capacity was also the largest of the three beams. The maximum load capacity of this beam is 249.12kN.

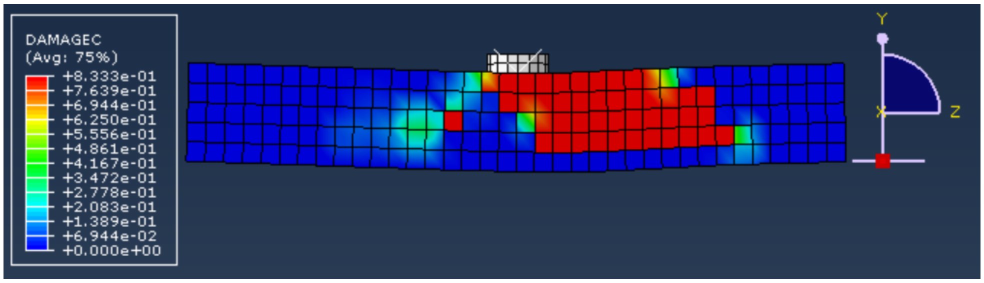

Fig. 5-29 *DAMAGEC of TBS*

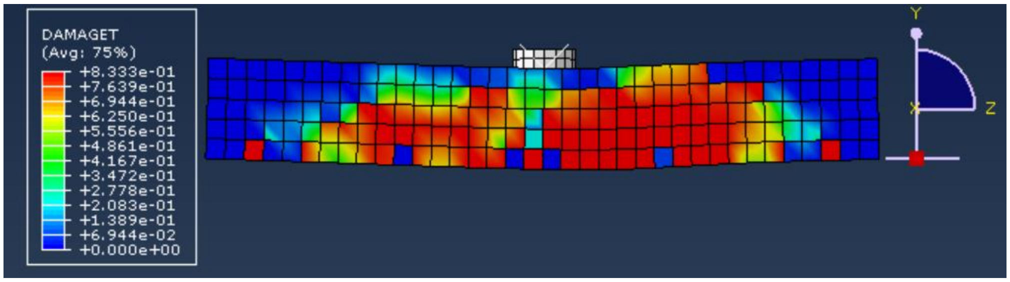

Fig. 5-30 *DAMAGET of TBS*

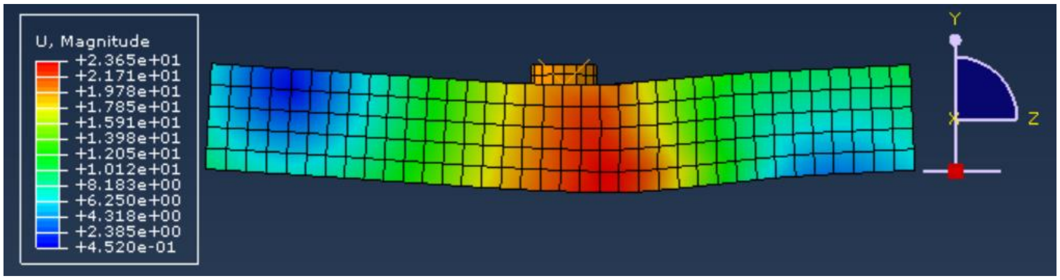

Fig. 5-31 *U, magnitude of TBS*

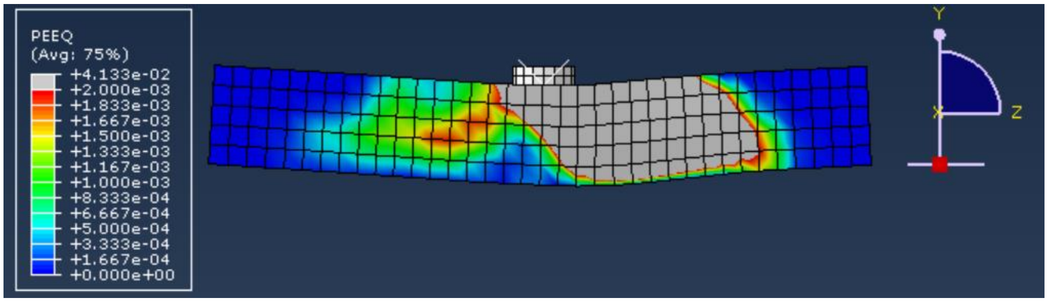

Fig. 5-32 *Equivalent Plastic Strain of TBS*

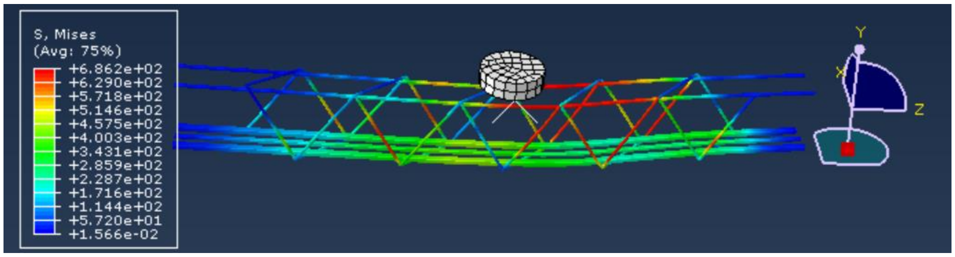

Fig. 5-33 *Von Mises stress of TBS*

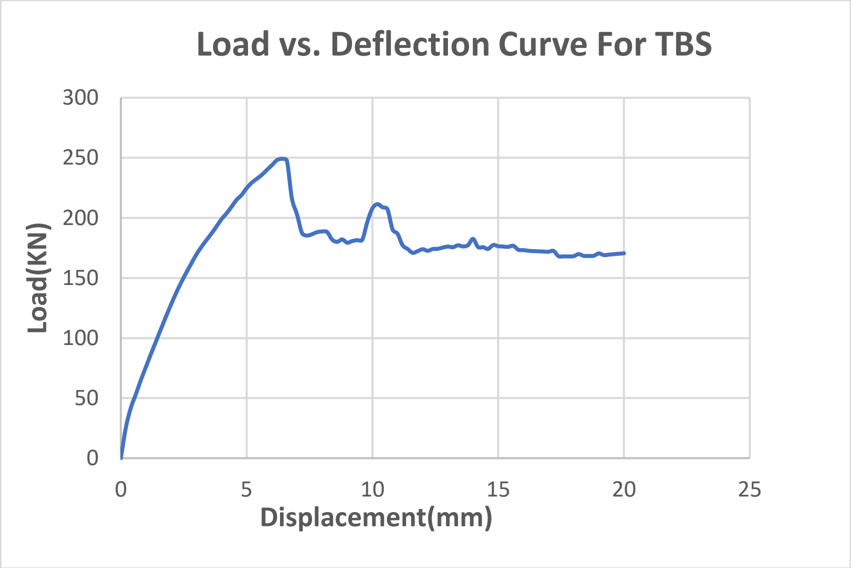

Fig. 5-34 *Load vs. mid-span deflection curve FEM TBS*

5.2.9. FEM Analysis of Truss Beam Non-Staggered (TBNS with 45^0 inclined)

From the TBNS beam, the FEM modelling noted a lower shear capacity than the FEM CB. The beam was failed in shear at ultimate load of 190.84kN.

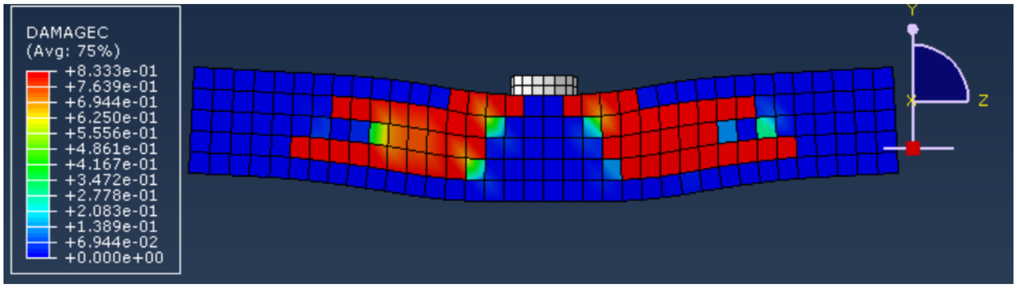

Fig. 5-35 *DAMAGEC of TBNS*

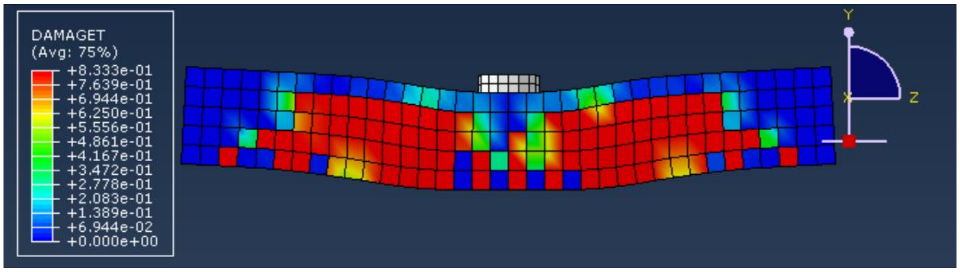

***Fig. 5-36** DAMEGET of TBNS*

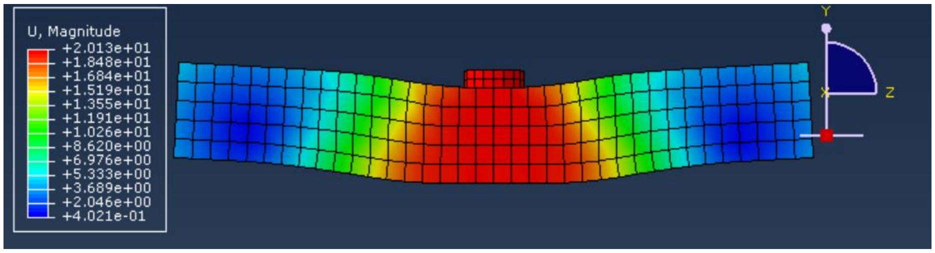

***Fig. 5-37** U, magnitude of TBNS*

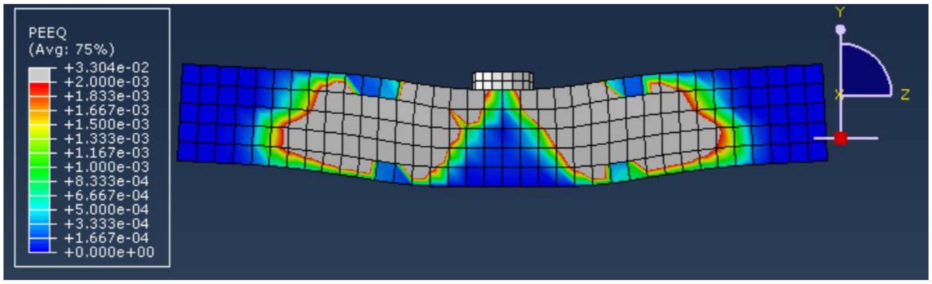

***Fig. 5-38** Equivalent Plastic Strain of TBNS*

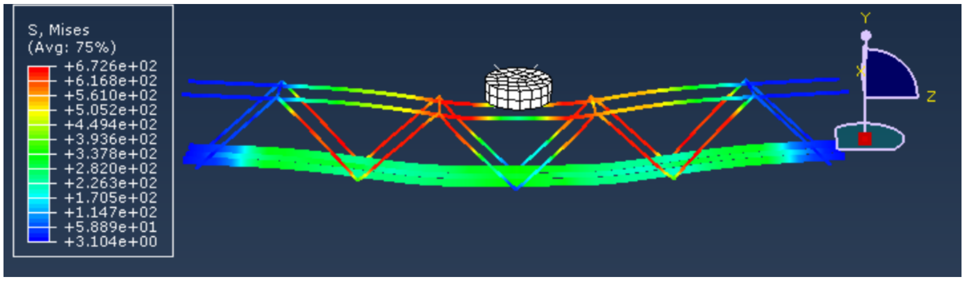

***Fig. 5-39** Von Mises stress of TBNS*

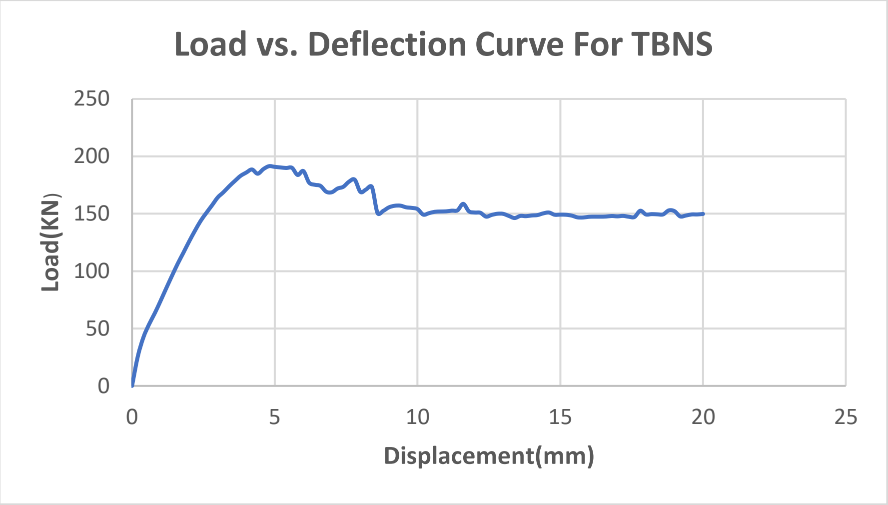

Fig. 5-40 *Load vs. mid-span deflection curve of FEM TBNS*

5.2.10. FEM Analysis of Truss Beam Staggered (TBS with 45^0 inclined)

From the TBS beam, the FEM modelling noted a lower shear capacity than the FEM CB. The beam was failed in shear at ultimate load of 201.8kN.

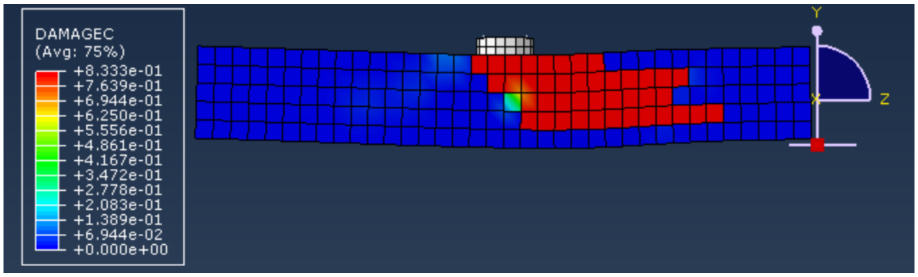

Fig. 5-41 *DAMAGEC of TBS*

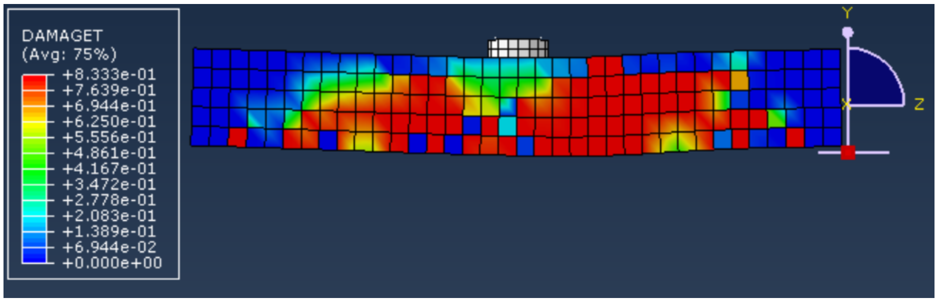

Fig. 5-42 *DAMAGET of TBS*

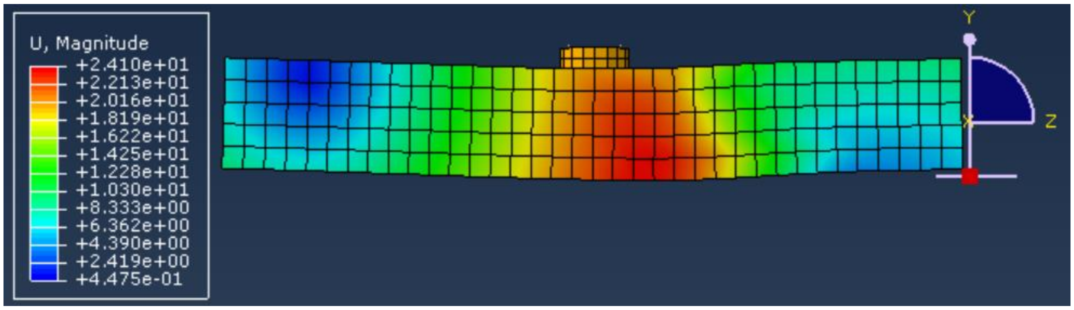

Fig. 5-43 *U, magnitude of TBS*

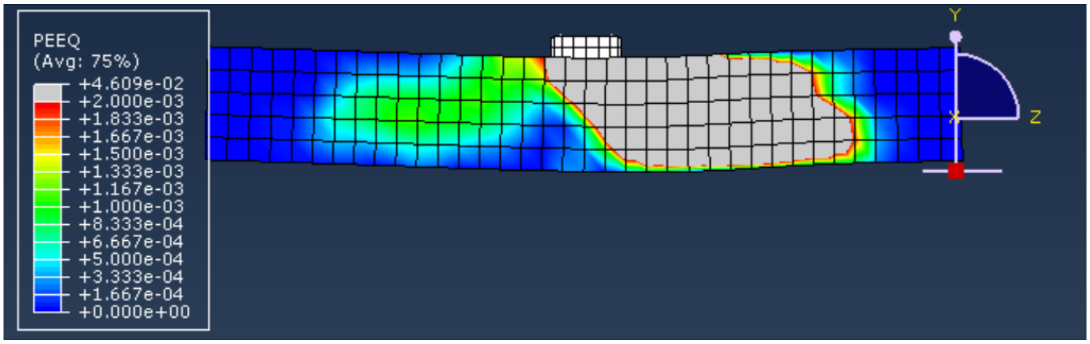

Fig. 5-44 *Equivalent Plastic Strain of TBS*

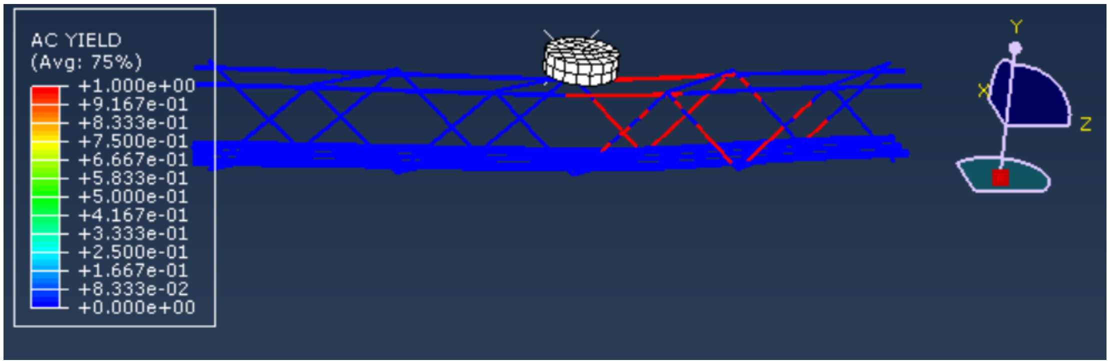

Fig. 5-45 *Von Mises stress of TBS*

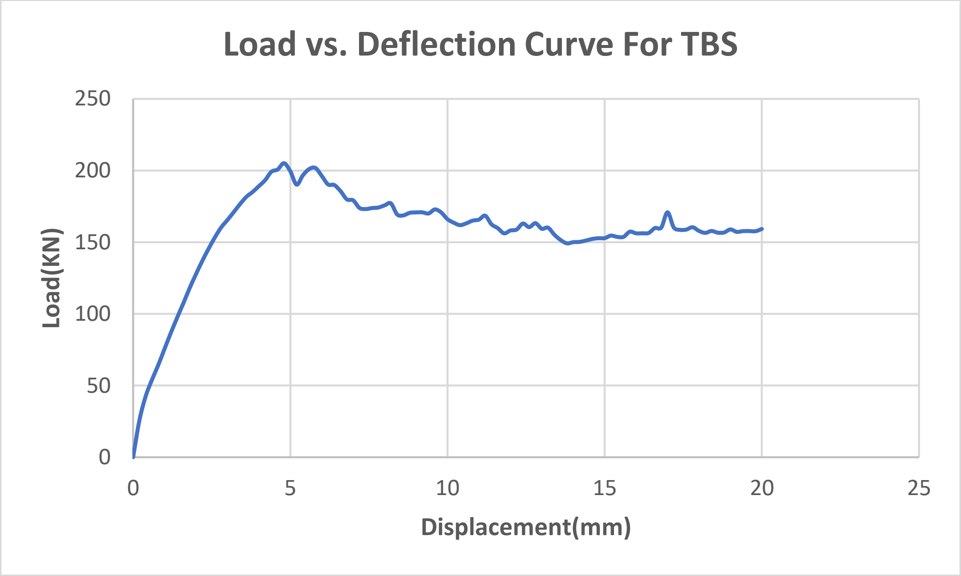

Fig. 5-46 *Load vs. mid-span deflection curve FEM TBS*

5.2.11. Comparison of All Results of FEM

Abaqus finite element method shows a smaller difference about 4kN in ultimate load capacity between the TBS (truss beam staggered) and TBNS (truss beam non-staggered) than what was observed experimentally around 18kN. While these differences in ultimate loads capacity could be associated with idealizations made within the Damage models, Boundary Conditions, Geometric Imperfections, Load Applications and changes in material properties. However, in terms of shear capacity, using the FEM and similar to the experimental work, represent the shear capacity of the beams as, TBNS(45^0) < TBS (45^0) < CB < TBNS(57^0) < TBS (57^0)

In slender beams with small cross sections, the effective depth and stirrup distribution are very important. When stirrups are inclined exactly 45^0, fewer stirrups may cross the diagonal crack due to geometry, this could reduce the effective shear capacity and cause instability or inefficacy and is more pronounced if spacing and anchorage are not adequate for those angles.

Inclined stirrups at angles that are slightly different from 45^0, such as 57^0, can cross more cracks and have a superior performance and therefore, additional stress dispersion. This is evident in

These results when indicated that the stirrup inclination of 57^0 produced optimal shear capacity results.

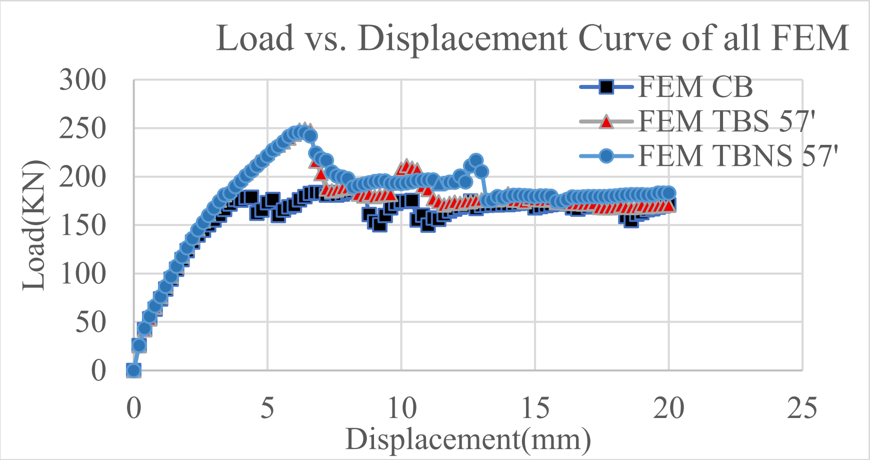

Fig. 5-47 *Load vs. mid-span deflection curve of all FEM*

5.3. Comparison of Experimental and FEM Results

In this section the Comparison of Experimental and FEM results of the beams are presented and discussed. Likewise, the experimental result, the finite element analysis result gives approximately the same crack patterns for all beams, but in an ultimate load capacity Likewise, the experimental result, the finite element analysis result gives approximately the same ultimate load capacity for TBNS, but in CB and TBS There was slightly difference in the ultimate loads Capacity between the experimental and FEM results These differences in ultimate loads Capacity can be associated with assumptions made within the Damage models, Boundary Conditions, Geometric Imperfections, Load Application and changes in material properties. Both approaches indicated that stirrup configuration is a significant shear stirrup configuration affecting shear capacity, with the staggered truss (TBS) outperforming the non-staggered (TBNS) and the reference (CB) beams.

5.3.1. Experimental and FEM of CB

The descriptions of the experimental control beam (EXP. CB) and Finite Element Method control beam (FEM CB) are as follows:

The crack patterns in both models are the same as shown in Fig. **5-49**. The ultimate load capacity of the EXP. CB is 210.5kN while that for the FEM CB is 187.45kN. The difference in ultimate load capacity is about 11% when comparing the experimental and simulation.

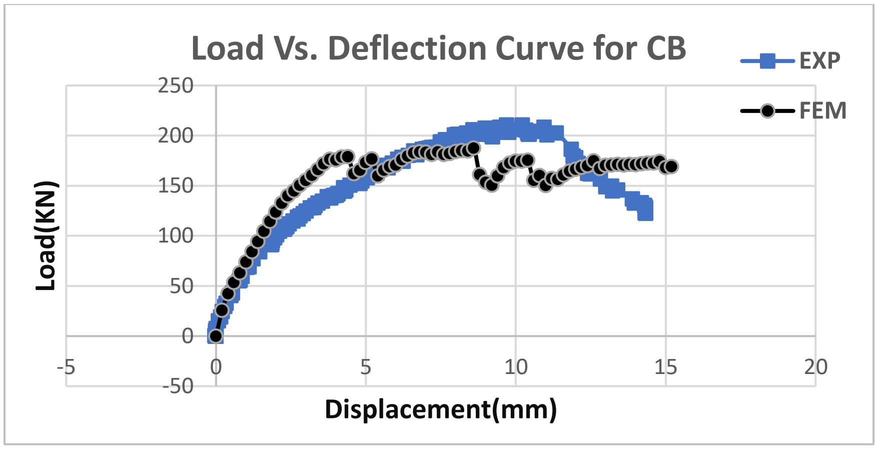

Fig. 5-48 *Load vs. mid-span deflection Curve of FEM and EXP. Of CB*

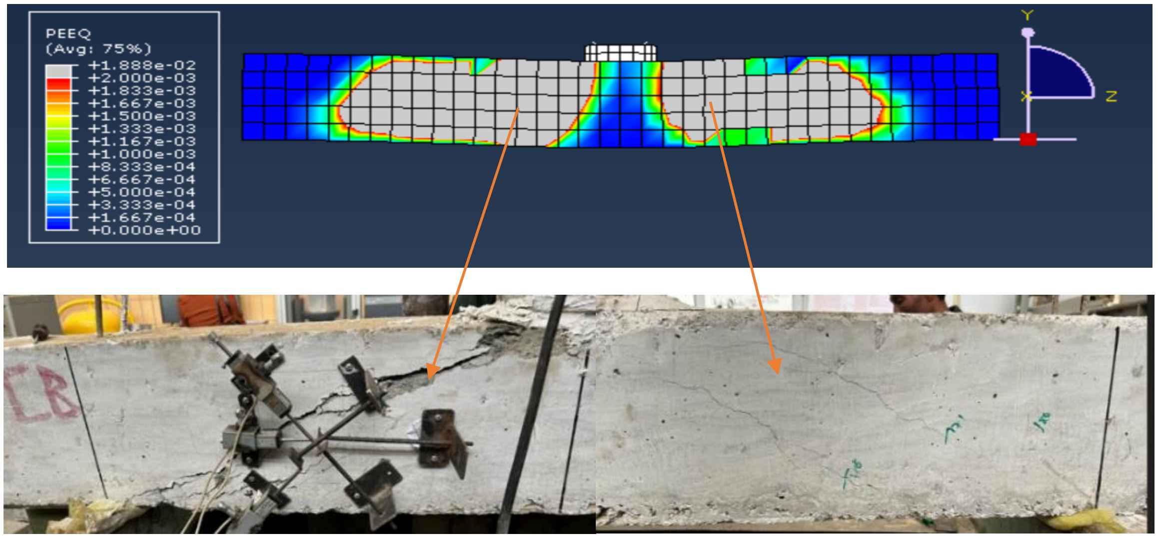

Fig. 5-49 *Damage locations of CB from FEM and EXP. Respectively*

5.3.2. Experimental And FEM of TBNS (57^0)

The analysis of the experimental (EXP. TBNS) versus the Finite Element Method (FEM TBNS) is as follows: The crack patterns were the same, as shown in fig. **5-50**. The experimental TBNS had an ultimate load capacity of 249.22kN, while the FEM TBNS had an ultimate load capacity of 245.74kN. This is a difference of around 1.44% between the experimental and the simulated load capacities.

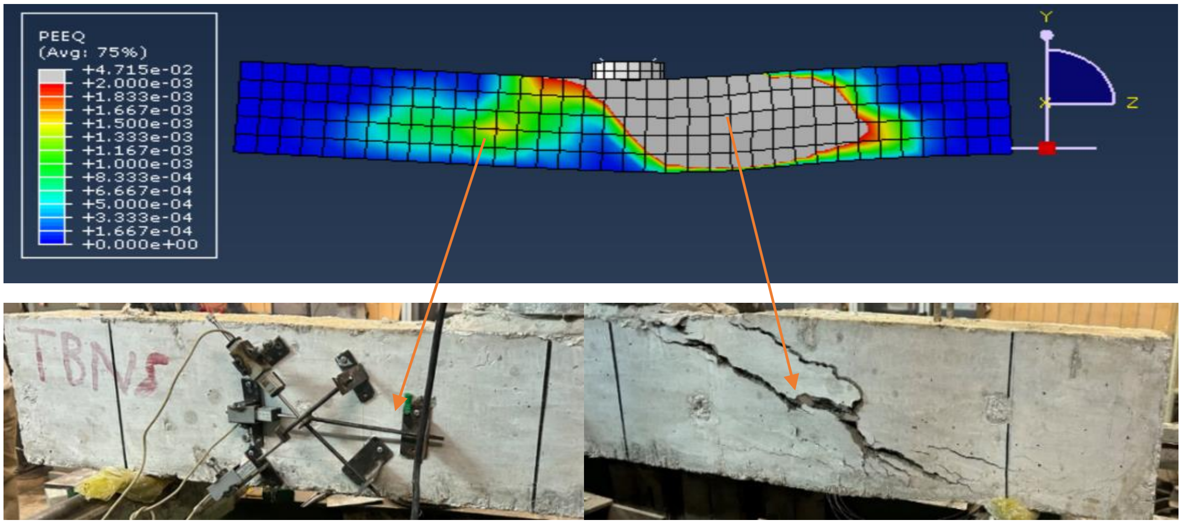

Fig. 5-50 *Damage locations of TBNS from FEM and EXP. respectively*

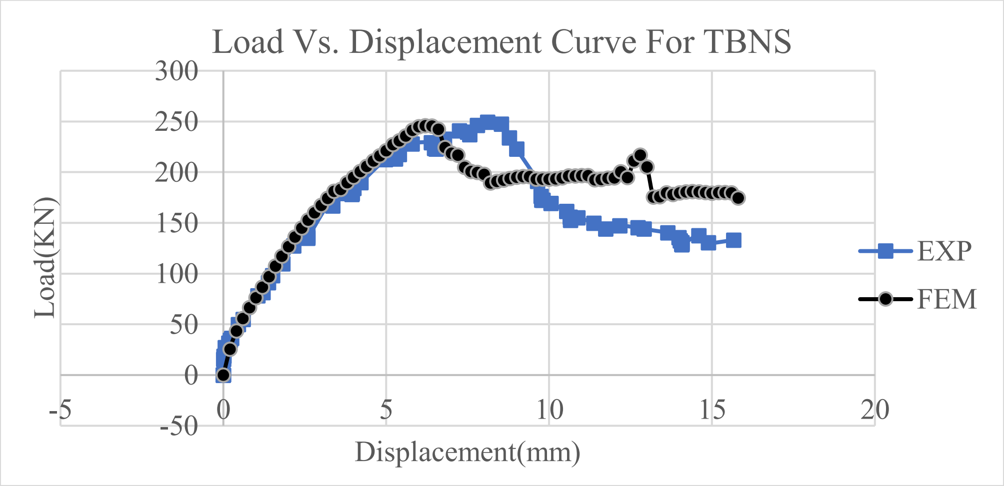

Fig. 5-51 *Load vs. mid-span deflection Curve of FEM and EXP. Of TBNS*

5.3.3. Experimental And FEM of TBS (57^0)

The comparison provides information regarding the crack patterns of the experimental TBS (EXP. TBS) and the Finite Element Method TBS (FEM TBS), which were the same as shown in Fig.**5-52**, and the ultimate load capacity of the EXP. TBS was 267kN, while the FEM TBS had an ultimate load capacity of 249.2kN. This gave a difference in terms of experimental to simulated load capacities of approximately 7.13%.

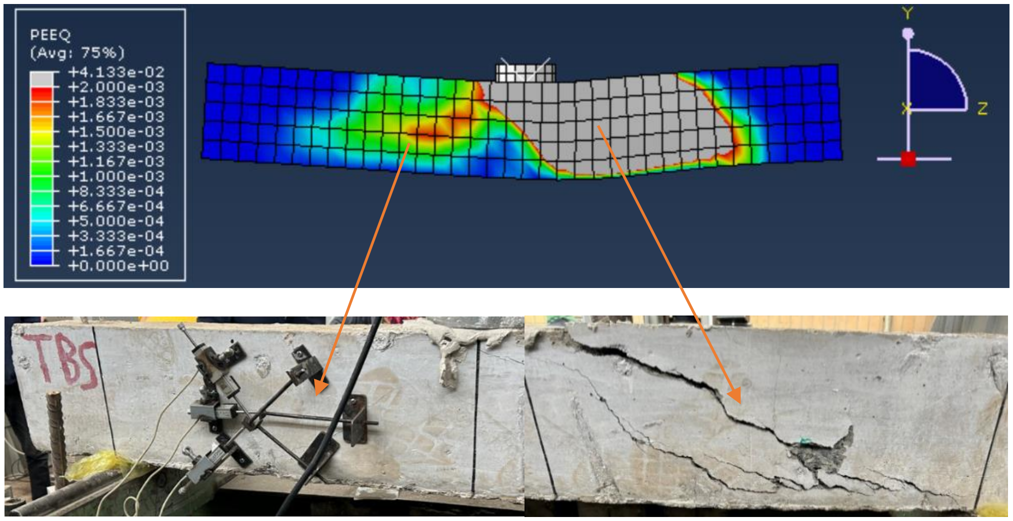

Fig. 5-52 *Damage locations of TBS from FEM and EXP. Respectively*

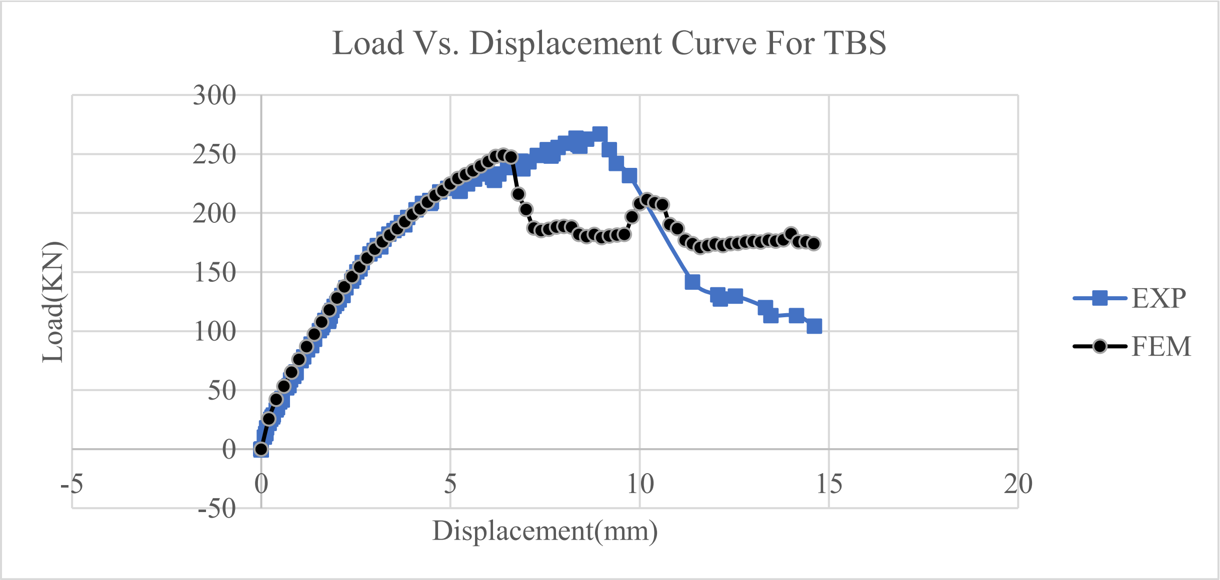

Fig. 5-53 *Load vs. mid-span deflection Curve of FEM and EXP. of TBS*

Table 5-1 Comparison of finite element and an experimental ultimate load of Specimens

Beam	P_{UEXP}KN	P_{UFEM}KN	P_{UEXP}KN/ P_{UFEM}KN
CB	210.5	187.45	1.123
TBNS (57^0)	249.22	245.74	1.014
TBS (57^0)	267.01	249.12	1.072

5.3.4. Discussion of A surface displacement measurement

5.3.4.1. Surface Shear Strain

The Geodatalog system recorded displacement information from each LVDT in mm units per one second interval. The displacement units were converted to strain units by dividing the recorded displacement (change in length) by the original length (170mm). Negative strain results are interpreted as compression and positive strain results are interpreted as tension. In this study, surface displacement measurements were only placed on the front left side of the beams to collect surface shear strain during loads. The tested beams, therefore, were Conventional Beam (CB), Truss Beam Non-Staggered (TBNS), and Truss Beam Staggered (TBS). The CB failure mode was the dominant shear crack on the front left side, consistent with where the surface shear measurement sensors were placed. Thus, the measured surface and horizontal strain response in the CB specimen was significant since the crack passed through the location of measurement.

For both TBNS and TBS, the dominant shear cracks developed in the front right side, which is not where the surface displacement sensors were placed on the left. This location difference resulted in lower surface and horizontal strains under applied loads for TBNS and TBS and may not have indicated the actual presence of dominant shear cracks. Surface shear strain is determined from the displacement data from the two diagonals set at angles of 45^o and 135^o, the difference in these values gives shear strain in the area of instrumentation defined grid, to calculate shear strain is critical to this area.

$$\epsilon_{x'} = \epsilon_x \cos^2\theta + \epsilon_y \sin^2\theta + \gamma_{xy} \sin\theta\cos\theta \text{.........6}$$

$$\epsilon_{y'} = \epsilon_x \sin^2\theta + \epsilon_y \cos^2\theta - \gamma_{xy} \sin\theta\cos\theta \text{.........7}$$

$$\gamma_{xy} = \frac{\epsilon_{x'} - \epsilon_x \cos^2\theta - \epsilon_y \sin^2\theta}{\sin\theta\cos\theta} \text{.........8}$$

5.3.4.2. Vertical Strain

Based on the defined surface measurement grid, vertical strain had to be calculated using strain relationship equations in Eq. 9 because an LVDT was not mounted in the vertical direction to directly measure. Using the diagonal strain at 45°, **ϵ**x from the LVDT which was mounted horizontally, and calculating ***γ***xy from 45° and 135° mounted measurements via the strain relationship equation below, **ϵ**y was established.

$$\epsilon_y = \frac{\epsilon_{x'} - \epsilon_x \cos^2\theta - \gamma_{xy} \sin\theta\cos\theta}{\sin^2\theta} \text{........9}$$

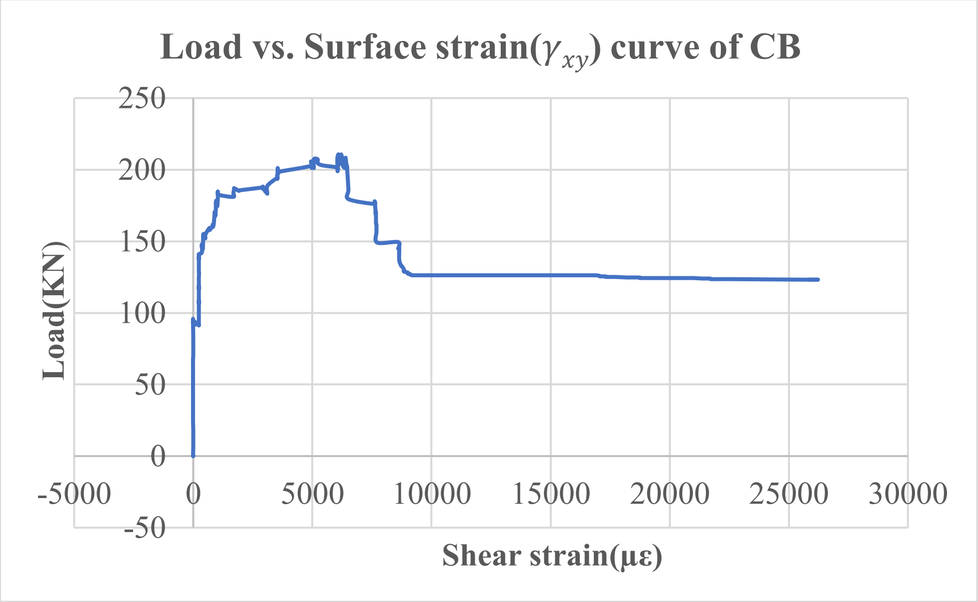

Fig. 5-54 *Load vs. Shear strain curve of CB*

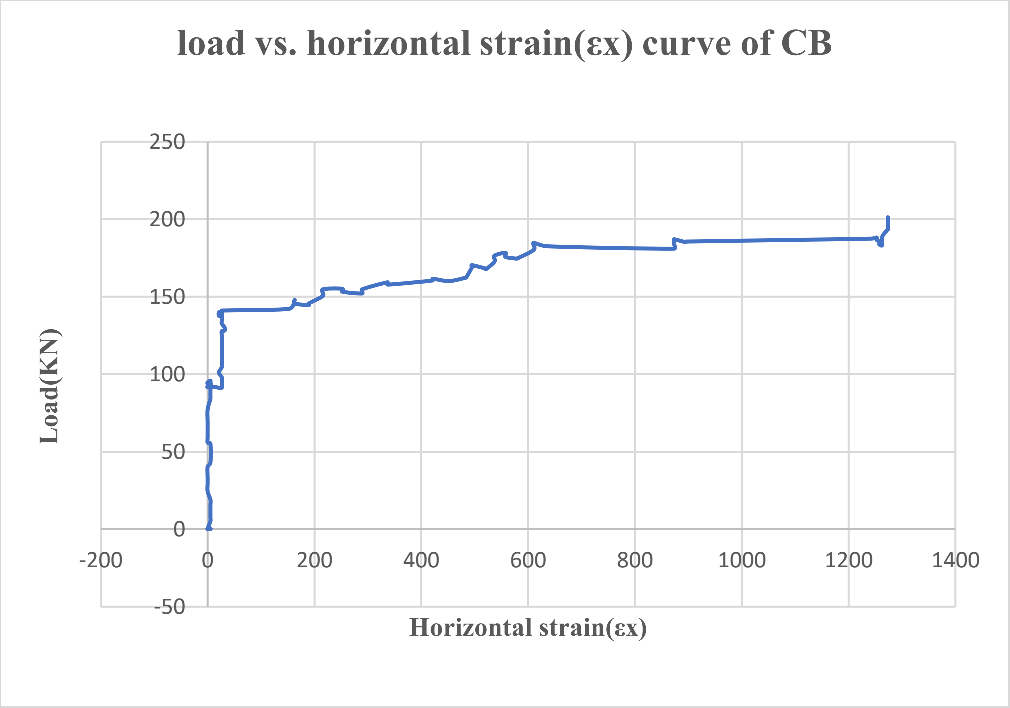

Fig 5-55 *Load vs. horizontal strain (εx) curve of CB*

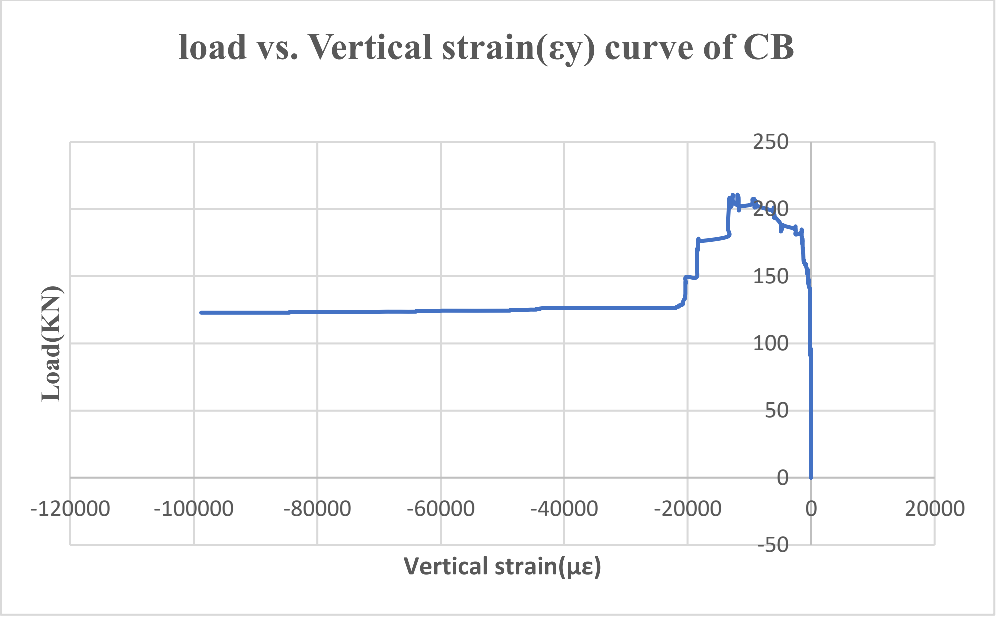

Fig 5-56 *Load vs. vertical strain(εy) curve of CB*

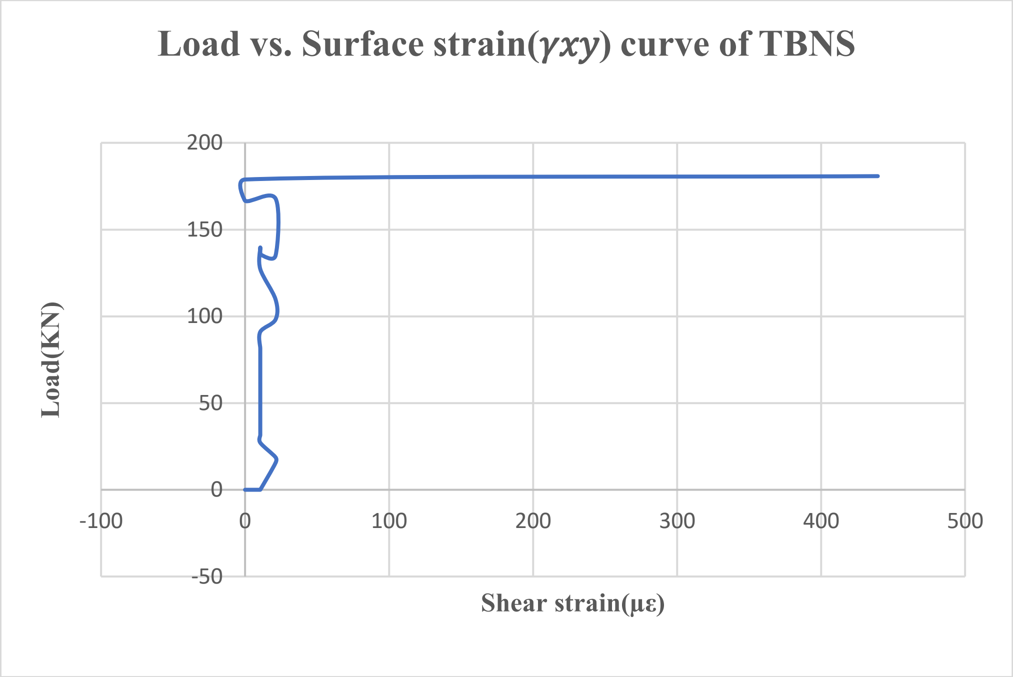

Fig 5-57 Load vs. Surface strain(𝛾𝑥𝑦) curve of TBNS

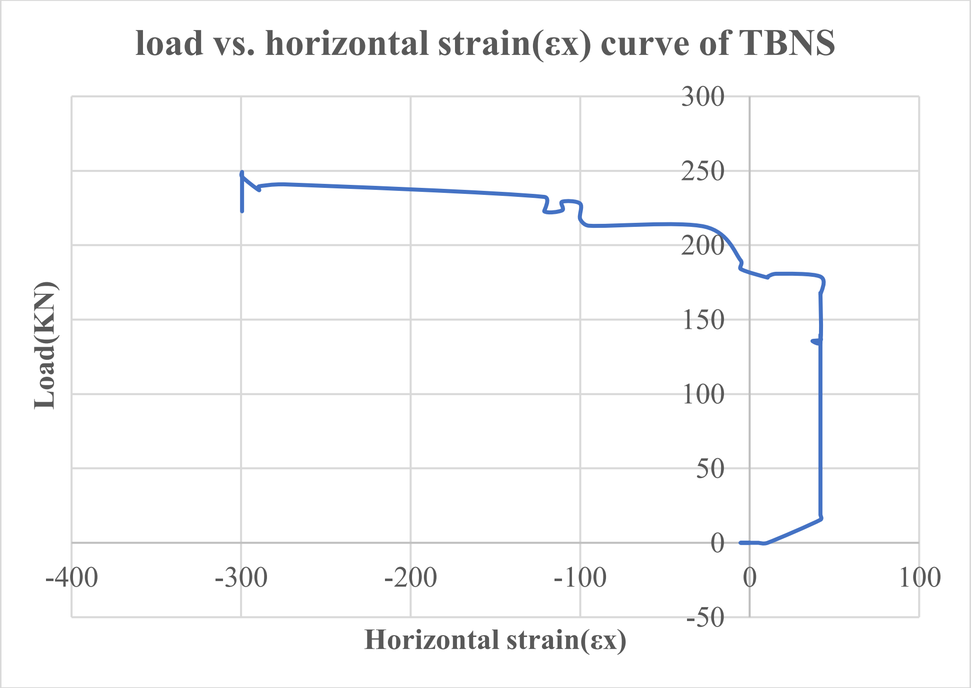

Fig 5-58 *Load vs. horizontal strain(εx) curve of TBNS*

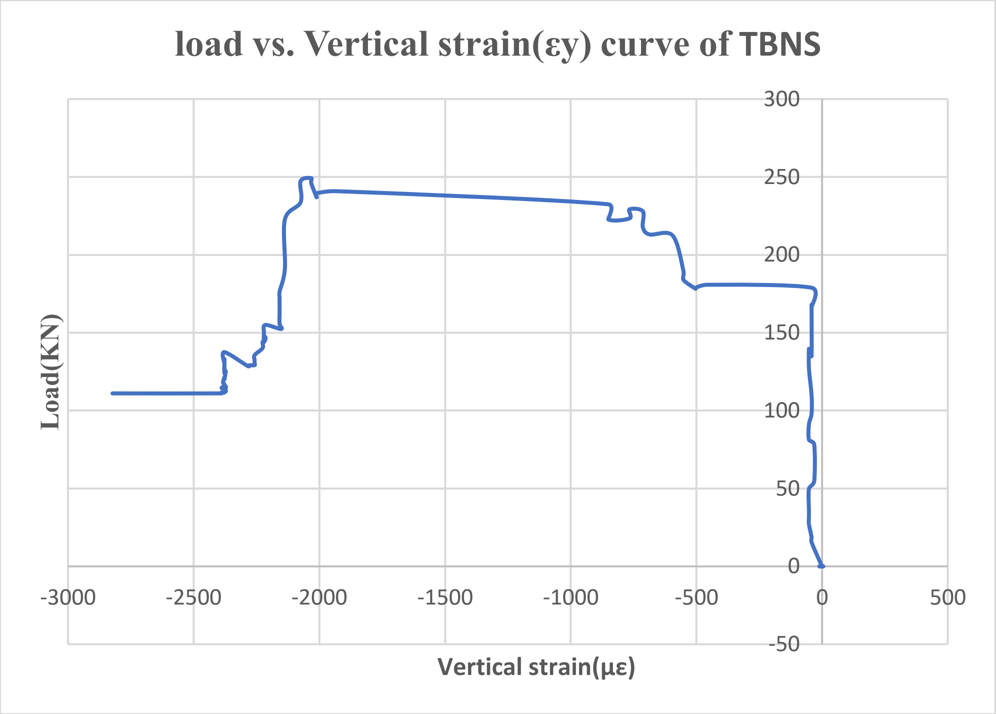

Fig 5-59 *Load vs. vertical strain(εy) curve of TBNS*

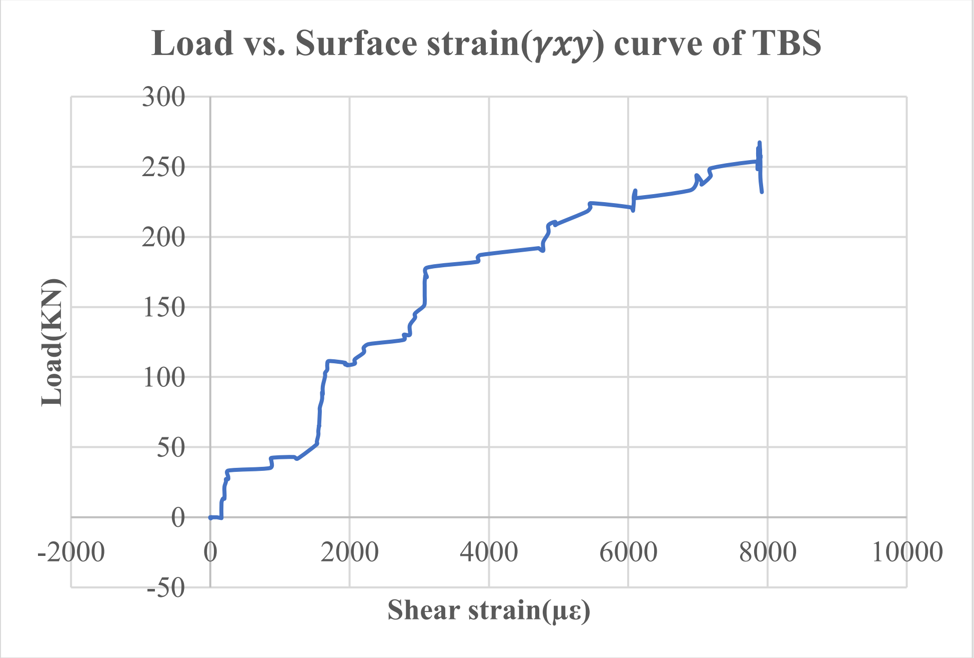

Fig 5-60 *Load vs. Surface strain(γxy) curve of TBS*

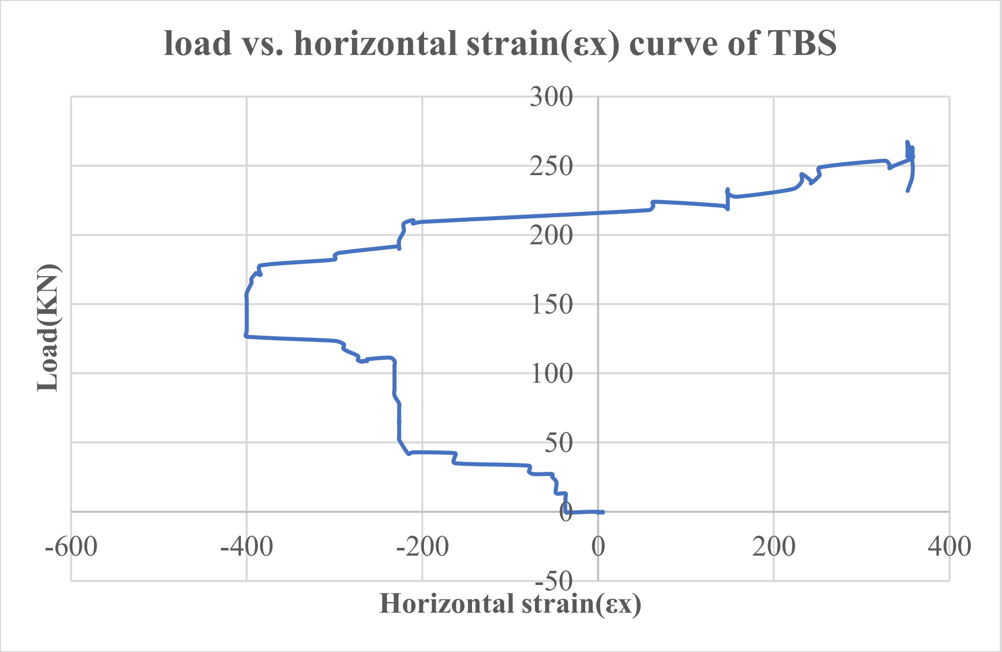

Fig 5-61 *Load vs. horizontal strain(εx) curve of TBS*

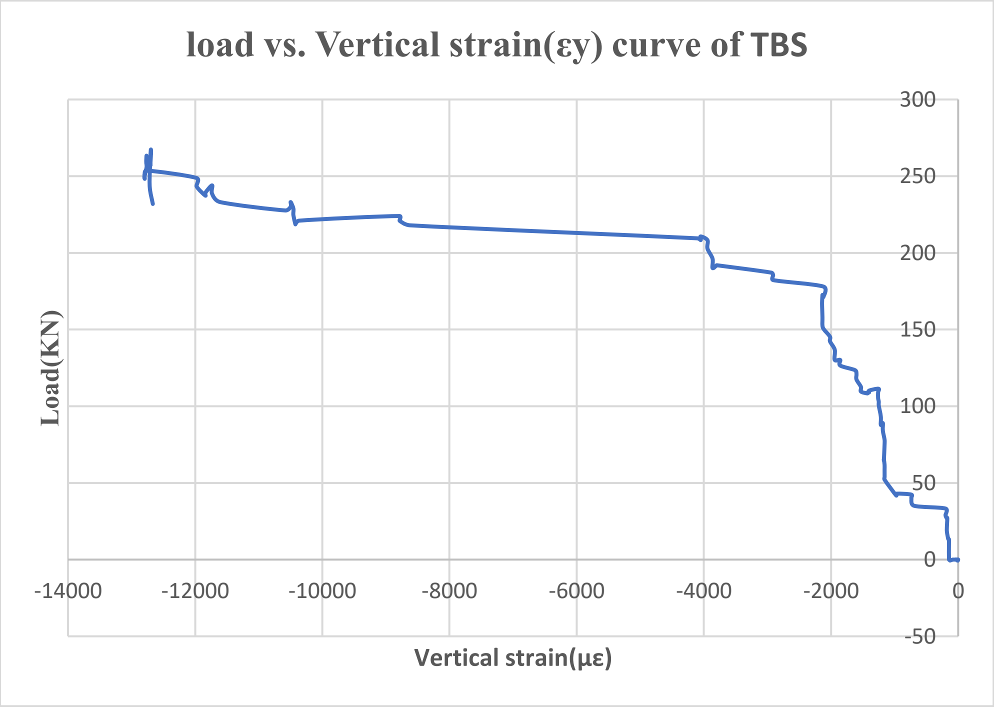

Fig 5-62 *Load vs. vertical strain(εy) curve of TBS*

CHAPTER SIX

6. CONCLUSION AND RECOMMENDATION

6.1. CONCLUSION

From the combined results of the experimental tests and finite element analysis (FEM) of the three stirrup arrangements, and the accompanying material properties, and reinforcement specifications, the following conclusions and suggestion made:

- All beams, regardless of stirrup arrangement, failed in shear mode in both the experimental and FEM investigations.
- The beams reinforced with a truss stirrup arrangement with (57^0) inclination, compared to the beams using conventional vertical stirrups, showed a greater ultimate shear strength, in both the experimental and FEM investigations.
- For the non-staggered truss type stirrup arrangement TBNS (57^0), there was an ultimate load capacity increase of approximately 18.25% in experimental tests, and 31.09% in FEM load capacity, noting an increase in shear resistance.
- Although the staggered Type stirrup arrangement TBS (57^0) was noted to have a greater improvement from the control beams, within experimental tests there was an ultimate load increase of about 26.75%, and 32.89% based on the FEM analysis of the same specimens. Overall, the TBS (57^0) truss stirrups were the most effective at improving shear strength.
- TBS (57^0) and TBNS (57^0) has the highest stiffness, and CB has the lowest stiffness.
- As noted in the analysis of shear strength, TBS and TBNS with a 45^0 exhibited a reduction in their effective shear strength compared to both FEM shear strength analysis and the testing data obtained for beams made from CB.
- Stirrup Configuration with Effective Inclination Notably Influence Shear Capacity and Easy of Concrete Casting.

6.2. RECOMMENDATION

1. Ultimately considering the improved shear capacity provided by truss stirrup configurations, particularly the staggered truss arrangement, these stirrup arrangements should be considered as a means of beam design to improve shear strength. This will ultimately provide structural elements that are safer, more effective with respect to load carrying capacity, and that are less congested with reinforcement.

2. As shear behavior of beams is influenced by several factors (longitudinal reinforcement ratio, shear span to depth ratio, size of the beam, concrete grade), there should be further work on the effect of spacing and arrangement of stirrups relative to these factors.

3. Due to the limitation of transducers available, surface shear was seen, and crack patterns were documented one side only. All observations relating to surface shear and crack patterning would achieve a fuller and more accurate picture if the transducer was placed on both sides to look at surface shear. Using the two will make the observations more accurate, and allow for the location of asymmetrical patterns which may be missed when monitoring the one side. Action needs to be taken to acquire or build additional transducers if both sides are to be tested again in future studies.

REFERENCE

1. James G. Macgregor, J.K.W., "Reinforced Concrete Mechanics and Design". New Jersey, US: Pearson Education, ed. Vol. 6. 2012. 108-109.

2. Grandić, D., "Shear resistance of reinforced concrete beams in dependence on concrete strength in compressive struts". Tehnicki vjesnik-Technical Gazette, 2015. 22(4): p. 925-934.

3. Mahzuz, H.M.A., Effectiveness of welded and trussed reinforcement in strength increment ofconcrete beams. 2021.

4. Juhin, W.J., et al., "Finite elemental assessment of torsional behavior of RC beams having different shear reinforcement". Building Engineering, 2024. 2(2).

5. Arafa, M., et al., "Performance of RC Beams with Embedded Steel Trusses Using Nonlinear FEM Analysis". Advances in Civil Engineering, 2018. 8(1): p. 1-8.

6. Afefy, H., et al., "Numerical Simulation of RC Beams Reinforced with Internal Steel Trusses". International Journal of Advances in Structural and Geotechnical Engineering, 2022. 03(02): p. 38-51.

7. Mohamed, N.F.Z.a.R.N., "The Effects of Inclined Shear Reinforcement in Reinforced Concrete Beam". 2018: p. 138-149.

8. Colajanni, P., et al., "Shear capacity in concrete beams reinforced by stirrups with two different inclinations". Engineering Structures, 2014. 81: p. 444-453.

9. Suhaimi, A.B., "inclined link as shear reinforcement in reinforced concrete beam" Faculty of Civil Engineering, 2015.

10. Rudy Djamaluddin, Y.B., Rita Irmawati, Abd. Madjid Akkas, Rusdi Usman Latief "Effect of the truss system to the flexural behavior of the external reinforced concrete beams" “International Journal of Civil, Environmental, Structural, Construction and Architectural Engineering", 2014. 8(6): p. 691-695.

11. Muneeb Ullah Khan, M.F., Khan Shahzada, "Shear Capacity Assessment of Reinforced Concrete Beams using Swimmer Bars as Shear Reinforcement". SSRG International Journal of Civil Engineering (SSRG-IJCE), 2015. 2(6): p. 14-20.

12. Deepika Dinesh, A., "Numerical Study of Hybrid Steel Trussed Concrete Beam". International Research Journal of Engineering and Technology (IRJET), 2017. 04(5): p. 1564-1568.

13. Sooryaprabha M Saju, S.U., "Study on Flexural Strength of Truss Reinforced Concrete Beams". International Research Journal of Engineering and Technology, 2016. 3(7): p. 1541-1545.

14. Nazia Sultana, A.A.N., Polleb Das, Md. Shamsul Hudha Chowdhury, Irfanul Islam, Kamrul Hasan and Md. Mehedi Hassan Masum, "Assessment of RC Beam Using Truss Pattern Shear Reinforcement". 2022. 6.

15. Pieter Laurens Frans, H.P., Rudy Djamaluddin, and Rita Irmawaty, "Effects of Truss System Reinforcements on Flexural Behavior of Reinforced Concrete Beams". International Journal of Engineering Science and Innovative Technology (IJESIT), 2019. 8(2).

16. Gungat, L., et al., "Finite Element Simulation and Analysis of RC Beams with Modified Stirrups". MATEC Web of Conferences, 2024. 397.

17. Piero Colajanni, S.P., Antonino Recupero, Nino Spinella, "Shear resistance analytical evaluation for RC beams with transverse reinforcement with two different inclinations". 2020.

18. Pinto, R.S., et al., "Influence of the supplementary reinforcement on the shear strength of beams with prefabricated truss stirrups". IBRACON Structures and Materiais, 2022. 15(1).

19. Reza Ghasemi, M. and A. Shishegaran, "Role of slanted reinforcement on bending capacity SS beams". Vibroengineering Procedia, 2017. 11: p. 195-199.

20. Moayyad M. Al-Nasra, N.M.A., "Shear Reinforcements in the Reinforced Concrete Beams". American Journal of Engineering Research (AJER), 2013. 2(10): p. 191-199.

21. Kishori, V. and Philip, V., "Effectiveness of swimmer bars as shear reinforcement in rectangular concrete beams". International Journal of Research in IT, Management and Engineering, 2014. 6(8): p. 45-51.

22. Demir, A., Caglar, N., Ozturk, H., and Sumer, Y., "Nonlinear finite element study on the improvement of shear capacity in reinforced concrete T-section beams by an alternative diagonal shear reinforcement". Engineering Structures, 2016. 120: p. 158-165.

23. British Standards Institution, "BS 882:1992 Specification for aggregates from natural sources for concrete", British Standards Institution, London, 1992. 3.

24. British Standards Institution (BSI), "BS EN 12390-3:2009, Testing Hardened Concrete - Compressive Strength of Test Specimens," London, United Kingdom, 2009.

25. Wosatko, A., Winnicki, A., Polak, M.A., and Pamin, J., "Role of dilatancy angle in plasticity based models of concrete". Archives of Civil and Mechanical Engineering, 2019. 19: p. 1268-1283.

26. Hafezolghorani, M., Hejazi, F., Vaghei, R., Jaafar, M. S. B., & Karimzade, K., "Simplified Damage Plasticity Model for Concrete," Structural Engineering International, 2017. 27(1): p. 68-78.

27. Allam, S.M., Shoukry, M.S., Rashad, G.E., Hassan, A.S., "Evaluation of tension stiffening effect on the crack width calculation of flexural RC members". Alexandria Engineering Journal, 2013. 52(2): p. 163-173.

28. European Committee for Standardization (CEN), "Design of Concrete Structures – Part 1-1: General Rules and Rules for Buildings," Eurocode 2, EN 1992-1-1, 2004.

29. Kent, D. C., and Park, R., "Flexural members with confined concrete." Journal of the Structural Division, ASCE, 1971. 97(7): p. 1969-1990.

30. Lubliner J, Oliver J, Oller S, & Onate E. A plastic-damage model for concrete. Int. J. Solids Struct. 1989; 25(3): 299–326

31. Kani, G., "Basic Facts Concerning Shear Failure," Journal of the American Concrete Institute, 1966. 63: p. 675-692.

32. ACI Committee 318, "Building Code Requirements for Structural Concrete (ACI 318-19) and Commentary (ACI 318R-19)," American Concrete Institute, Farmington Hills, MI, USA, 2019.

33. Japan Society of Civil Engineers (JSCE), "Guidelines for Concrete No.3. Structural Performance Verification. Standard Specification for Concrete Structures-2002," Tokyo, Japan, 2002.

34. Comité Européen de Normalisation, "Eurocode 2: Design of Concrete Structures. Part 1–1: General Rules and Rules for Buildings (EN-1992-1-1)," Brussels, Belgium, 2004.

35. Ahmad, Gasham, et al., "Alternative shear cracking strength equation for reinforced concrete normal beams without stirrups". Iraqi Journal of Civil Engineering, 2011. 8(1): p. 44-49.

36. Bukhari, S. N., & Ahmad, S. (2007). "Effect of shear span ratio on the failure mechanism and shear strength of reinforced concrete beams". SSRG International Journal of Civil Engineering, 2(6), 14-20.

37. "Simplified Shear Design of Structural Concrete Members: Appendixes," Simpl. Shear Des. Struct. Concr. Members Append., vol. 78, no. July, 2005.

38. Hunegnaw, C. B., & Wondimu, T. (2021). "Effect of orientation of stirrups in combination with shear span to depth ratio on shear capacity of RC beams". Research Article. Issued on October 19, 2021.

39. Tesfaye, K. "An Experimental Investigation on the Effect and Mechanism of Side Cover Spalling for Slender Beams Subjected to Shear". MSc Thesis, Addis Ababa University May 2021.

APPENDEX

APPENDEX A

Design of beam

Dimension of beam and other specifications

- Total beam length = 1.75m
- Clear span of beam =1.35m
- Depth of beam= 260mm
- Width of beam = 170mm
- Concrete cover = 25mm
- Stirrup's diameter = 8mm
- Longitudinal bar in one row(bottom) = 20mm (two number of bars) and 14mm (one number of bar)
- Longitudinal bar in one row(top) = 10mm (two number of bars)

Initial data and Material strength

$$d' = cc + ∅s + ∅l/2 = 25 + 8 + 20/2 = 43mm$$

$$d = D - d' = 260 - 43 = 217mm$$

Ratio of shear span to effective depth=av/d=0.675/0.217=3.11 is a slender beam

Actual **As** (longitudinal tension bars) = 628.28 mm^2 (2∅20) & 153.94 mm^2 (1∅14) total = 782.22 mm^2

Concrete	**Rebar**
C-30Mpa	$f_{ylong.tension}$=602.3MPa
	f_{yw}=652MPa

Back analysis of beam by using the actual specification of materials the maximum moment capacity of the beam

$Md, s = 76.24\ KNm$

M=PL/4---p=4M/L=76.24*4/1.35=226KN

The design value of the shear resistance is given in Eurocode 2, EN 1992-1-1, 2004 as follows

$C_{Rd,\,c}=0.18/\gamma_c=0.18/1.5=0.12$

$V_{Rd,c} = [C_{Rd,c}k(100 * \rho_1 f_{ck})^{1/3} + k_1\sigma_{cp}]\bar{b_w}d \leq [V_{min} + k_1\sigma_{cp}]b_w d$

Where: f_{ck} is in MPa

$C_{Rd,\,c}=0.18/\gamma_c=0.18/1.5=0.12$

$k = 1 + \sqrt{\frac{200}{d}} = 1 + \sqrt{\frac{200}{217}} = 1.96 \leq 2.0$....................OK (Take k=1.96)

$\rho = {}^{A_{st}}/_{d*b_w} = 0.02 \leq 0.02$…………………OK (Take ρ=0.02)

$V_{min} = 0.035 * k^{\frac{3}{2}} * f_{ck}^{\frac{1}{2}} = 0.035 * 1.96^{\frac{3}{2}} * 30^{\frac{1}{2}} = 0.526$

$$\sigma_{cp} = \frac{N_{ED}}{A} = 0$$

A_{st}	is the area of the tensile reinforcement, which extends $\geq(f_{cd} + d)$ beyond the section considered
b_w	is the smallest width of the cross-section in the tensile area[mm]
N_{ED}	is the axial force in the cross-section due to loading[N]
A_c	is the area of concrete cross-section[mm^2]
$V_{Rd,c}$	in [N]

Thus the design value for shear resistance will be:

$$V_{Rd,c} = [C_{Rd,c}k\,(100 * \rho_1 fck)^{1/3} + k_1\sigma_{cp}]\,b_w d \geq [V_{min} + k_1\sigma_{cp}]b_w d$$

$$V_{Rd,c} = [0.12 * 1.96\,(100 * 0.013 * 20)^{1/3} + 0.15 * 0] * 170 * 217 = 34kN$$

$$V_{Rd,c(min)} = [V_{min} + k_1\sigma_{cp}]b_w d = [0.526 + 0.15 * 0] * 170 * 217 = 19kN$$
$$< 34\text{KN} \ldots\ldots\ldots\ldots\ldots\ldots\ldots\ldots. OK!$$

$$= 1 + \sqrt{\frac{200}{d}} \leq 2$$

$$z = 0.9d = 195.3\text{mm}$$

$$\rho = {}^{A_{st}}/_{d*b_w} = 0.02 = 0.02\ldots\text{ok}$$

$V_{Rd,s} = A_{sw}{*}zf_{ywd}\cot\theta/S$ =100.53*195.3*652*1/200=64KN, Use $\theta=45^0$

$V_{Rd,max} = [\alpha_c v_1 f_{cd}/(\cot\theta + \tan\theta)]b_w z$

$v_1 = 0.6(1 - f_{ck}/250)$ =0.526

$\alpha_{c=1}$

$V_{Rd,max}$=181KN so take the minimum of $V_{Rd,max}$ and $V_{Rd,s}$ We take 64KN

So $V_{Rd} = V_{Rd,c} + V_{Rd,s}$ =34KN + 64KN=98KN

Total load of shear force= 2*(34KN + 64KN) = 196 kN

Total load of bending= $226\ KN$>196 kN Fail in shear

Where:

- $V_{Rd,c}$- design shear resistance of the member without shear reinforcement
- ϱ_1- Tensile reinforcement ratio
- b_w- the smallest width of the cross-section in the tensile area
- d- effective depth
- z- distance from location of compressive stress resultant to centroid of tension steel
- A_{s1}- area of tensile reinforcement
- $V_{Rd,s}$- design shear capacity with vertical shear reinforcement
- f_{ywd}- yield strength of web reinforcement
- A_{sw}- cross sectional area of shear reinforcement
- $V_{Rd,max}$- maximum shear force sustained by a member limited by crushing of the compression strut
- α_c -a coefficient for the interaction of the stress in the compression chord and any applied axial compressive stress
- θ-the angle between concrete compression strut and main tension chord

APPENDEX B

Material Test Property of rebar

specimen no.	Diameter		Length (mm)	yield load (Mpa)	Failure load (Mpa)	Average yield load (Mpa)	Average Failure load (Mpa)	Elongation (%)
	D1(mm)	D2(mm)						
8(1)	7.36	8.53	60	668.47	728.16	652.55	711.24	30.00
8(2)	7.39	8.54	60	636.64	694.33			
10(1)	9.44	11.21	60	659.56	757.60	660.19	754.42	23.00
10(2)	9.34	11.29	60	660.83	751.23			
14(1)	13.28	15.08	60	622.35	716.54	624.30	723.36	21.43
14(2)	13.46	14.14	60	626.24	730.19			
20(1)	19.15	21.94	60	574.88	667.83	580.30	673.56	21.50
20(2)	19.21	21.94	60	585.71	679.29			

Rebar tensile test result

Specimen	**Average Yield Strength (MPa)**	**Average Ultimate Strength (MPa)**	**Elongation (%)**
$\phi 8$	653	711	30
$\phi 10$	660	754	23
$\phi 14$	624	723	21
$\phi 20$	580	673	22

APPENDEX C

Material Test Property of concrete ingredients

Sieve analysis of River sand

Sieve (mm)	**Weight Retained (g)**	**Percent Retained (%)**	**Pass (%)**	**Specification Limit BS**	
				Lower Limit	**Upper Limit**
37.5					
19					
14	0	0	100	100	100
10	15	0	100	100	100
5	82	3	97	90	100
2.36	214	7	90	60	100
1.18	503	16	73	30	90
0.6	1144	37	36	15	54
0.3	914	30	6	5	40
0.15	176	6	1		
0.075	8	0	0		
Pan	8	0			
Total	**3,064**				

Material properties of river sand

River sand Material Properties	
Bulk Specific Gravity	2.32
Bulk Specific Gravity (SSD)	2.38
Apparent Specific Gravity	2.45
Water Absorption	3.58
Clay Lumps and Friable Particles	0.2
Unit weight, loose kg/m3	1,350

Unit weight, Rodded kg/m3	1,450
Soundness (Using Sodium Sulphate), %	3
Sand Equivalent, %	88

Sieve analysis of crushed sand

Size	**Weight Retained(g)**	**Percent Retained**	**Pass**	**Specification Limit BS**	
(mm)		**(%)**	**(%)**	**Lower Limit**	**Upper limit**
37.5					
19					
14			100	100	100
10	0	0	100	100	100
5	38	3	97	90	100
2.36	120	10	87	60	100
1.18	310	26	61	30	90
0.6	410	34	27	15	54
0.3	130	11	16	5	40
0.15	103	9	8		
0.075	60	5	3		
Pan	36	3			
Total	**1,207**				

Material properties of crushed sand

Crushed sand Material Properties	
Bulk Specific Gravity	2.73
Bulk Specific Gravity (SSD)	2.84
Apparent Specific Gravity	2.86
Water Absorption	2.8
Clay Lumps and Friable Particles	0
Unit weight, loose kg/m3	1,500
Unit weight, Rodded kg/m3	1,660
Soundness (Using Sodium Sulphate), %	2
Sand Equivalent, %	84

Sieve analysis of Coarse aggregate 01

Size (mm)	**Weight Retained (g)**	**Percent Retained (%)**	**Pass (%)**	**Specification Limit BS**	
				Lower Limit	**upper Limit**
37.5					
19			100	100	100
14	0	0	100	100	100
10	330	11	89	85	100
5	2121	72	16	0	25
2.36	468	16	0		5
1.18	4	0			0
0.6	1	0			
0.3	1	0			
0.15	2	0			
0.075	2				
Pan	2				
Total	**2,931**				

Material properties of Coarse aggregate 01

Coarse aggregate 01 Material Properties	
Bulk Specific Gravity	2.74
Bulk Specific Gravity (SSD)	2.84
Apparent Specific Gravity	2.87
Water Absorption	1.7
Clay Lumps and Friable Particles	
Unit weight, loose kg/m3	1,520
Unit weight, Rodded kg/m3	1,640
Soundness (Using Sodium Sulphate), %	1
Sand Equivalent, %	

Sieve analysis of coarse aggregate 02

Size (mm)	**Weight Retained (g)**	**Percent Retained (%)**	**Pass (%)**	**Specification Limit BS**	
				Lower Limit	**Upper Limit**
25	0	0	100	100	100
19	600	12	88	85	100

14	2780	56	32	0	70
10	1450	29	2	0	25
5	100	2	0.1	0	5
2.36	2	0	0		
1.18	0	0			
0.6	0	0			
0.3	0	0			
0.15	0	0			
0.075	3				
Pan	0				
Total	**4,935**				

Material properties of Coarse aggregate 02

Coarse aggregate 02 Material Properties	
Bulk Specific Gravity	2.77
Bulk Specific Gravity (SSD)	2.84
Apparent Specific Gravity	2.9
Water Absorption	1.2
Clay Lumps and Friable Particles	
Unit weight, loose kg/m3	1,530
Unit weight, Rodded kg/m3	1,650
Soundness (Using Sodium Sulphate), %	1
Sand Equivalent, %	

APPENDEX D

Experimental load vs. displacement data of CB

disp. (mm)	load(KN)	disp. (mm)	load(KN)	disp. (mm)	load(KN)	disp. (mm)	load(KN)
0.00	0.00	1.86	93.17	6.07	176.44	11.85	186.32
0.00	0.00	1.86	93.17	6.21	178.34	11.92	179.48
0.00	0.00	1.86	92.78	6.23	175.68	11.93	176.05
0.00	0.00	1.86	92.78	6.24	174.53	12.00	177.96
0.00	0.00	1.86	92.40	6.25	174.53	12.09	172.26
0.00	0.00	1.86	92.40	6.42	180.24	12.10	169.22
-0.01	0.00	1.86	92.02	6.60	184.80	12.30	170.35
0.00	0.00	1.86	92.02	6.68	182.52	12.40	162.36
-0.01	0.00	1.86	92.02	6.71	181.00	12.48	161.61

0.00	0.00	1.85	91.65	6.77	183.66	12.83	156.66
0.00	0.39	1.86	91.65	6.89	186.32	13.01	149.06
-0.02	0.39	1.86	91.65	7.00	187.08	13.20	149.44
-0.02	0.39	1.86	91.26	7.02	185.18	13.23	144.88
-0.02	0.39	1.89	95.44	7.06	185.56	13.40	145.63
-0.02	0.39	1.93	97.73	7.11	187.47	13.90	136.89
-0.02	0.39	1.96	98.10	7.20	188.22	13.96	132.71
-0.02	0.39	2.03	101.15	7.21	186.70	14.19	133.09
-0.02	0.39	2.12	104.56	7.22	185.56	14.30	130.42
-0.02	0.39	2.26	108.38	7.23	184.80	14.32	128.90
-0.02	0.39	2.28	107.23	7.23	184.04	14.33	128.15
-0.02	0.39	2.29	106.47	7.23	183.66	14.33	127.38
-0.02	0.39	2.30	106.86	7.23	183.28	14.33	127.00
-0.02	0.39	2.33	108.38	7.33	188.60	14.33	126.63
-0.02	0.39	2.37	109.51	7.48	193.55	14.33	126.24
-0.02	0.39	2.44	111.79	7.53	193.55	14.33	126.24
-0.02	0.39	2.57	114.84	7.66	195.82	14.33	125.86
-0.02	0.39	2.72	118.64	7.70	193.55	14.33	125.48
-0.02	0.39	2.74	116.73	7.75	195.07	14.33	125.48
-0.02	0.39	2.81	119.77	7.95	200.77	14.33	125.11
-0.02	0.39	2.92	122.07	8.06	201.16	14.33	125.11
-0.02	0.39	3.01	124.72	8.14	199.25	14.33	125.11
-0.02	0.39	3.15	127.76	8.17	197.34	14.33	124.72
-0.02	0.39	3.26	128.15	8.23	198.49	14.33	124.72
-0.02	0.39	3.31	130.05	8.36	202.68	14.33	124.72
-0.02	0.39	3.40	132.71	8.57	205.72	14.33	124.34
-0.02	0.39	3.56	134.61	8.65	203.43	14.33	124.34
-0.02	0.39	3.71	139.17	8.67	201.16	14.33	124.34
-0.01	5.32	3.79	137.65	8.74	203.05	14.33	123.96
0.01	7.61	3.83	137.65	8.77	201.53	14.33	123.96
0.08	15.21	3.91	139.93	8.79	201.16	14.33	123.96
0.15	19.01	3.94	140.32	8.98	207.24	14.33	123.59
0.21	24.34	4.00	140.32	9.12	207.24	14.33	123.59
0.29	29.66	4.03	141.07	9.15	204.57	14.33	123.59
0.34	32.70	4.07	142.21	9.17	203.05	14.33	123.59
0.50	40.31	4.26	147.92	9.18	201.91	14.33	123.59
0.55	42.97	4.29	145.63	9.20	201.16	14.33	123.59
0.78	55.14	4.29	144.50	9.21	200.01	14.33	123.20
0.81	55.89	4.33	145.63	9.21	199.64	14.33	123.20

0.87	59.70	4.48	150.58	9.23	198.87	14.33	123.20
1.05	68.45	4.66	154.76	9.29	203.05	14.33	123.20
1.11	69.21	4.78	155.14	9.47	208.38	14.33	123.20
1.24	77.19	4.80	153.24	9.69	210.66	14.33	122.82
1.45	84.04	4.81	152.10	9.74	206.47	14.33	122.82
1.46	84.04	4.86	154.76	9.76	204.57	14.33	122.82
1.66	93.54	5.02	159.32	9.77	203.05	14.33	122.82
1.82	95.82	5.05	157.80	9.86	206.10	14.33	122.82
1.82	94.69	5.13	160.47	10.22	210.66	14.33	122.82
1.82	93.92	5.25	161.61	10.33	205.34	14.33	122.82
1.82	93.54	5.26	160.09	10.40	202.68	14.33	122.44
1.82	92.78	5.30	162.36	10.43	201.16	14.33	122.44
1.82	92.40	5.37	162.36	10.46	201.16	12.55	71.49
1.82	92.02	5.55	168.83	10.62	204.20	9.75	14.82
1.82	92.02	5.70	170.35	10.95	208.38	8.24	1.14
1.82	91.65	5.74	168.07	11.04	200.77	8.03	0.00
1.85	93.92	5.74	167.70	11.36	202.68	7.98	0.00
1.85	93.54	5.88	172.63	11.36	202.68	7.93	0.00

Experimental load vs. displacement data of TBNS

disp. (mm)	load(KN)	disp. (mm)	load(KN)	disp. (mm)	load(KN)	disp. (mm)	load(KN)
0.00	0.00	6.38	229.20	16.00	126.55	18.79	112.34
0.00	0.00	6.48	223.40	16.82	128.48	18.79	112.34
0.00	0.00	6.53	222.76	16.99	123.97	18.79	111.71
0.00	0.00	6.78	232.44	17.87	125.26	18.79	111.71
0.00	0.00	7.25	240.84	18.16	120.09	18.80	111.71
0.00	0.00	7.49	239.53	18.51	121.38	18.79	111.71
0.00	0.00	7.57	236.95	18.59	118.80	18.80	111.71
0.01	15.50	7.79	246.00	18.63	117.51	18.80	111.71
0.01	18.73	8.11	249.22	18.64	116.87	18.79	111.71
0.06	27.12	8.53	247.28	18.66	116.22	18.80	111.71
0.16	31.65	8.78	233.73	18.66	115.56	18.80	111.71
0.21	34.23	9.00	222.76	18.67	115.56	18.79	111.71
0.26	36.16	9.65	191.11	18.67	115.56	18.80	111.71
0.46	49.72	9.75	176.27	18.67	114.93	18.80	111.71
0.60	54.89	9.77	172.38	18.71	114.93	18.80	111.71
1.06	78.13	9.81	172.38	18.73	114.93	18.79	111.71

1.22	81.35	10.05	169.16	18.74	114.29	18.79	111.71
1.39	91.05	10.54	161.41	18.74	114.29	18.79	111.71
1.51	98.14	10.64	155.61	18.74	114.29	18.79	111.05
1.83	109.76	10.65	152.37	18.74	114.29	18.80	111.05
2.16	127.20	10.89	154.96	18.74	113.64	18.80	111.05
2.57	139.46	11.38	149.79	18.74	113.64	18.80	111.05
2.59	137.53	11.74	143.97	18.74	113.64	18.79	111.05
2.59	136.22	12.17	147.21	18.74	113.64	18.80	111.05
2.60	135.59	12.73	145.28	18.74	113.64	18.80	111.05
2.59	134.95	12.92	143.97	18.74	112.98	18.80	111.05
3.21	167.87	13.64	140.12	18.74	112.98	18.80	110.40
3.36	166.58	13.99	135.59	18.74	112.98	18.80	111.05
3.65	178.86	14.02	132.37	18.74	112.98	18.80	111.05
3.90	180.78	14.07	130.42	18.74	112.98	18.80	111.05
3.95	178.86	14.07	130.42	18.74	112.98	18.80	111.05
3.95	178.20	14.07	129.13	18.74	112.98	9.48	-6.46
4.01	184.02	14.08	129.13	18.74	112.34	9.41	-6.46
4.22	189.82	14.07	128.48	18.74	112.34	9.37	-6.46
4.98	212.43	14.07	128.48	18.74	112.34	9.35	-6.46
5.28	213.07	14.59	137.53	18.74	112.34	9.34	-6.46
5.40	217.59	14.89	130.42	18.74	112.34	9.33	-6.46
5.79	227.93	15.66	133.01	18.79	112.34	9.31	-6.46

Experimental load vs. displacement data of TBS

disp. (mm)	load(KN)	disp. (mm)	load(KN)	disp. (mm)	load(KN)	disp. (mm)	load(KN)
0.00	0.00	1.41	93.24	5.26	218.57	19.34	85.97
0.00	-0.61	1.54	100.50	5.46	224.61	19.45	83.55
0.00	0.00	1.59	102.93	5.64	228.86	19.49	82.34
0.00	-0.61	1.63	105.35	5.99	233.11	19.52	82.34
0.00	-0.61	1.68	108.98	6.11	230.07	19.55	81.73
0.00	0.00	1.78	111.40	6.16	227.65	19.56	81.13
0.00	-0.61	1.78	110.19	6.28	233.11	19.56	81.13
0.00	0.00	1.78	108.98	6.51	238.55	19.56	81.13
0.00	0.00	1.78	108.98	6.86	243.99	19.56	80.53
0.00	0.00	1.78	108.37	6.90	239.14	19.56	81.13
0.00	0.00	1.79	109.59	6.92	237.34	19.56	80.53
0.00	0.00	1.83	112.61	7.08	243.39	19.56	80.53

0.00	0.00	1.87	117.46	7.30	248.83	19.56	80.53
0.00	0.00	1.93	121.09	7.56	253.67	19.56	79.92
0.00	0.00	1.99	123.51	7.66	250.66	19.56	80.53
0.00	0.00	2.07	126.55	7.66	248.23	19.56	80.53
0.00	-0.61	2.13	130.16	7.71	250.06	19.56	79.92
0.00	-0.61	2.16	130.16	7.85	255.50	19.56	79.92
0.00	0.00	2.24	136.83	8.04	259.13	19.56	79.92
0.00	0.00	2.39	142.27	8.32	263.36	19.56	79.92
0.00	0.00	2.44	145.31	8.37	257.92	19.56	79.92
0.08	10.30	2.52	150.15	8.40	257.92	19.64	79.92
0.12	13.32	2.61	152.57	8.42	256.71	19.65	79.92
0.12	13.32	2.67	158.03	8.60	262.76	19.65	79.31
0.15	18.16	2.87	165.30	8.96	267.01	19.64	79.92
0.21	21.80	2.98	168.31	9.20	253.67	19.64	79.31
0.25	25.43	3.07	172.56	9.38	242.18	19.64	79.92
0.28	27.25	3.13	172.56	9.73	231.88	19.64	79.92
0.31	27.25	3.16	171.33	11.40	141.67	19.64	79.92
0.32	29.06	3.24	178.00	12.06	130.78	19.64	79.31
0.39	33.29	3.38	182.25	12.13	127.14	19.64	79.92
0.43	35.12	3.51	185.27	12.53	129.57	19.64	79.31
0.49	39.96	3.60	187.09	13.33	119.88	19.64	79.31
0.54	42.38	3.70	191.93	13.47	113.21	19.64	79.31
0.55	42.98	3.76	191.93	14.15	113.21	19.64	79.31
0.56	41.78	3.80	190.11	14.62	104.14	19.64	79.31
0.68	52.07	3.87	196.16	14.73	104.14	19.64	79.31
0.73	53.89	4.09	202.82	15.41	101.10	19.64	79.31
0.78	58.74	4.26	208.27	15.74	97.49	19.64	79.31
0.86	61.76	4.45	210.70	15.80	95.06	19.64	79.31
0.92	65.39	4.47	208.27	16.60	95.66	19.64	79.31
0.92	64.77	4.50	209.48	16.95	93.24	19.64	79.31
1.05	75.08	4.72	217.96	17.10	94.45	19.64	79.31
1.13	78.11	4.93	221.00	17.54	94.45	19.64	79.31
1.22	84.15	5.13	224.02	18.09	90.22	11.52	-10.30
1.32	88.99	5.22	221.00	18.22	90.22	11.48	-10.30
1.33	87.80	5.25	218.57	18.82	84.76	11.47	-10.30